AD NUMBER

AD820391

LIMITATION CHANGES

TO:

Approved for public release; distribution is unlimited.

FROM:

Distribution authorized to U.S. Gov't. agencies and their contractors; Critical Technology; AUG 1967. Other requests shall be referred to Rome Air Development Center, Attn: EMLI, Griffiss AFB, NY 13441-5700. This document contains export-controlled technical data.

AUTHORITY

RADC ltr, 17 Sep 1971

RADC-TR-67-305

MICROWAVE PHASE MEASUREMENTS ON THE ACTIVE SWEPT FREQUENCY INTERFEROMETER RADAR SYSTEM

Vaughn K. Grace, Captain, USAF

TECHNICAL REPORT NO. RADC-TR-67-305
August 1967

Rome Air Development Center
Air Force Systems Command
Griffiss Air Force Base, New York

When US Government drawings, specifications, or other data are used for any purpose other than a definitely related government procurement operation, the government thereby incurs no responsibility nor any obligation whatsoever; and the fact that the government may have formulated, furnished, or in any way supplied the said drawings, specifications, or other data is not to be regarded, by implication or otherwise, as in any manner licensing the holder or any other person or corporation, or conveying any rights or permission to manufacture, use, or sell any patented invention that may in any way be related thereto.

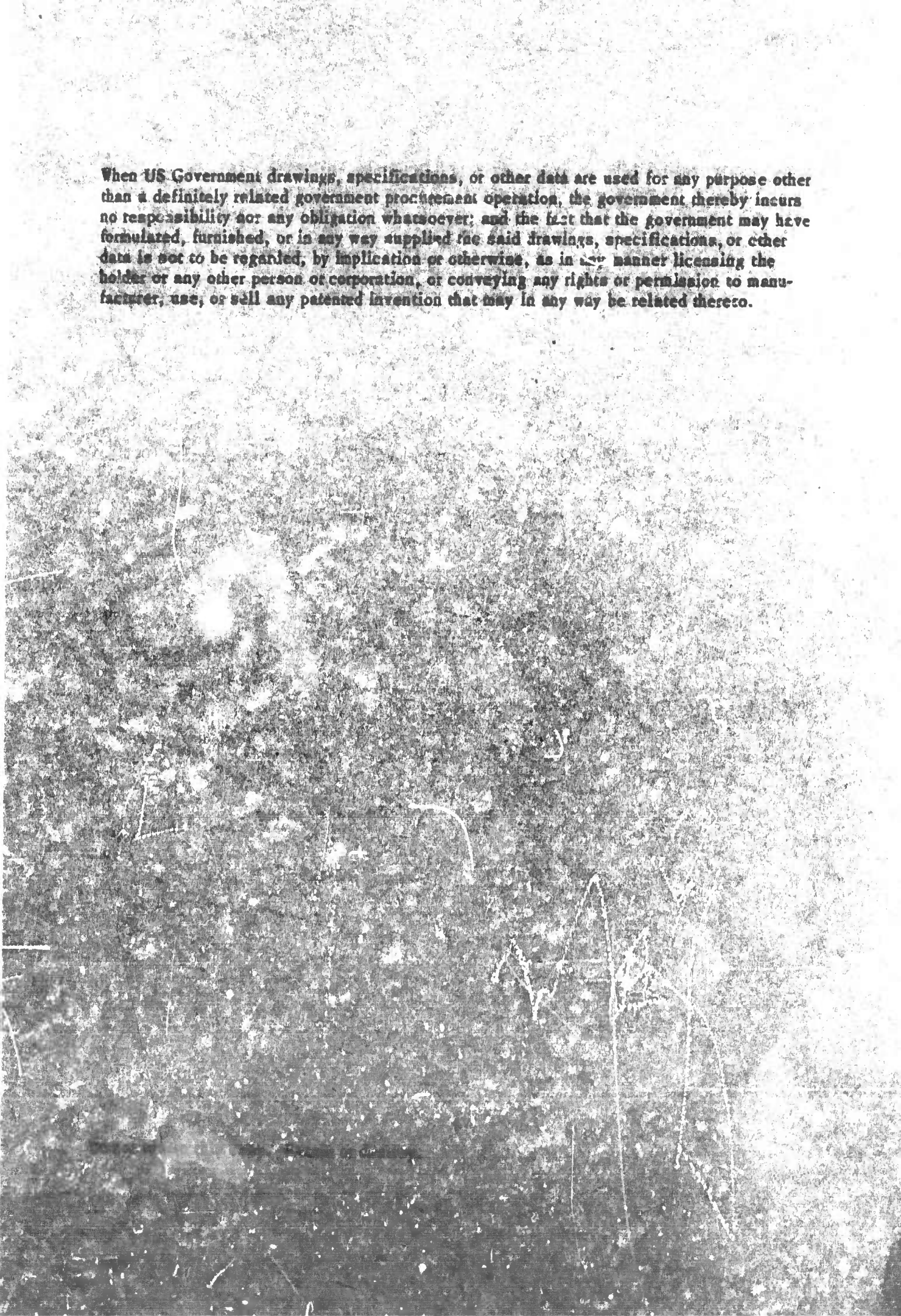

MICROWAVE PHASE MEASUREMENTS ON THE ACTIVE SWEPT FREQUENCY INTERFEROMETER RADAR SYSTEM

Vaughn K. Grace, Captain, USAF

AFLC, GAFB, N.Y., 27 Sep 67-73

FOREWORD

The research and testing described in this report were accomplished under Project 6512.

Captain Grace transferred into the Air Force after graduating from the United States Naval Academy at Annapolis. He received his Master's degree at Oklahoma State University in 1963 and was then assigned to Rome Air Development Center. Captain Grace was a project officer for the Active Swept Frequency Interferometer Radar, concerned with phase linearity problems and phase measurements. He received his captaincy in December 1965. In August 1966 he was assigned to Oklahoma State University to work toward his doctorate under the AFIT program.

This technical report has been reviewed by the Foreign Disclosure Policy Office (EMLI). It contains information embargoed from release to Sino-Soviet Bloc countries by AFR 400-10, "Strategic Trade Control Program" and, therefore, is not releasable to the Clearinghouse for Scientific and Technical Information.

This technical report has been reviewed and is approved.

Approved: JOSEPH FALLIK
Ch, Space Surv & Instr Branch
Surveillance & Control Division

Approved: THOMAS S. BOND, JR.
Colonel, USAF
Ch, Surveillance and
Control Division

FOR THE COMMANDER:
IRVING J. GABELMAN
Chief, Advanced Studies Group

ABSTRACT

Many microwave systems currently in operation require strict control of the phase and gain characteristics of the system. The Active Swept Frequency Interferometer Radar system transmits a linear FM ramp to obtain range and angle information. If the transfer characteristics of the system transmission and receiving networks possess constant gain and linear phase variation over the signal frequency band, the linear FM ramp signal will pass through the system undistorted. If, however, the system possesses inadequate phase linearity, the signal suffers phase distortion which results in a loss of signal amplitude and range resolution.

The various methods of measuring phase linearity and associated errors are discussed, as well as results of actual tests conducted on the components of the experimental Active Swept Frequency Interferometer Radar. These tests include results with passive components, as well as active components such as TWTs and high power klystrons.

TABLE OF CONTENTS

TABLE OF CONTENTS (Cont)

LIST OF ILLUSTRATIONS

LIST OF ILLUSTRATIONS (Cont)

SECTION I

INTRODUCTION

Many microwave systems currently in operation require strict control of the phase and gain characteristics of the system. The Active Swept Frequency Interferometer Radar (ASFIR) system transmits a linear FM ramp to obtain range and angle information. If the transfer characteristics of the system transmission and receiving networks possess constant gain and linear phase variation over the signal frequency band, the linear FM ramp signal will pass through the system undistorted. If, however, the system possesses inadequate phase linearity, the signal suffers phase distortion which results in a loss of signal amplitude and range resolution.

Minimizing phase distortion and phase instabilities are of concern not only in chirp radar systems, but also in broadband television systems, communication systems, and steerable phased array antennas. This report deals with phase distortion and phase instabilities.

To adequately describe the phase linearity of a system, highly accurate phase data is required. This report discusses the problems, on a system basis, of obtaining phase linearity data with an accuracy of better than 1 degree. Having achieved the required accuracy, the report then discusses methods of minimizing phase distortion and phase instabilities in a radar system.

Quantative field test data on a microwave system containing parametric amplifiers, traveling-wave tube amplifiers, a high power klystron amplifier, coaxial cables, waveguide runs, directional couplers, multiplexers, bends, transitions, isolators, and mixers is presented and discussed. Although the test data recorded primarily phase vs. frequency characteristics of the test devices; phase versus other parameters, such as power and time, are also presented.

In achieving minimum phase distortion and phase instability, certain system operating conditions are required. These conditions will be discussed, as well as techniques for tuning certain active devices for most linear phase versus frequency response.

SECTION II
DISCUSSION

Phase measurements were made on the transmission and receiving components of the ASFIR (Active Swept Frequency Interferometer Radar) system during initial two-site configuration and during final three-site configuration. Two modes of signal transmission are used to obtain target information in the ASFIR system, CW and FM. A pulsed constant-frequency signal of 2.4 milliseconds maximum duration is transmitted to obtain target radial velocity information. The FM mode involves the transmission of a pulsed linearly varying frequency in order to obtain target range and angle information. Frequency is swept linearly over a maximum frequency band of 48.6 MHz centered at 3 GHz. Maximum pulse length is 2.4 milliseconds.

A simplified block diagram of the ASFIR system is given in Figure 1. Monostatic operation utilizes only the components located at the master site. The echo return at the master site is amplified in an S-band receiver chain and mixed with a delayed replica of the transmitted signal to obtain an IF (intermediate frequency) signal. The IF signal is processed and a coherent memory filter performs a Fourier analysis on the signal. The coherent memory filter performs simultaneous frequency analyses over its entire frequency coverage and its output is presented as a deflection-modulated oscilloscope display showing the amplitude of all Fourier components on a calibrated frequency axis. All target parameters in the frequency domain are determined from the coherent memory filter output display.

Multistatic operation utilizes both master and slave sites simultaneously. The echo return received at the master site is processed in a manner similar to that for monostatic operation.

The echo returns received at the slave sites are amplified through low noise r-f amplifiers, mixed with pump signals having nominal frequencies of 7 GHz, and the resulting sum signals and pump signals are relayed by microwave links to the master site. At the master site, the pump and sum signals are recombined to produce an exact replica of the signals received at the remote sites. These signals are mixed with delayed coherent replicas of the transmitted signal, and the resulting IF signals are processed, then analyzed by coherent memory filters.

If the transfer characteristics of the transmission and receiving networks possess constant gain and linear phase variation over the signal frequency band, the FM signal will pass through the system undistorted. If, however, the system does not possess constant gain and linear phase variation over the signal frequency band, the signal will be distorted. The amplitude characteristic is of less importance since the attendant non-linearity of the phase characteristic introduces a greater signal distortion for a given amplitude distortion.[1]

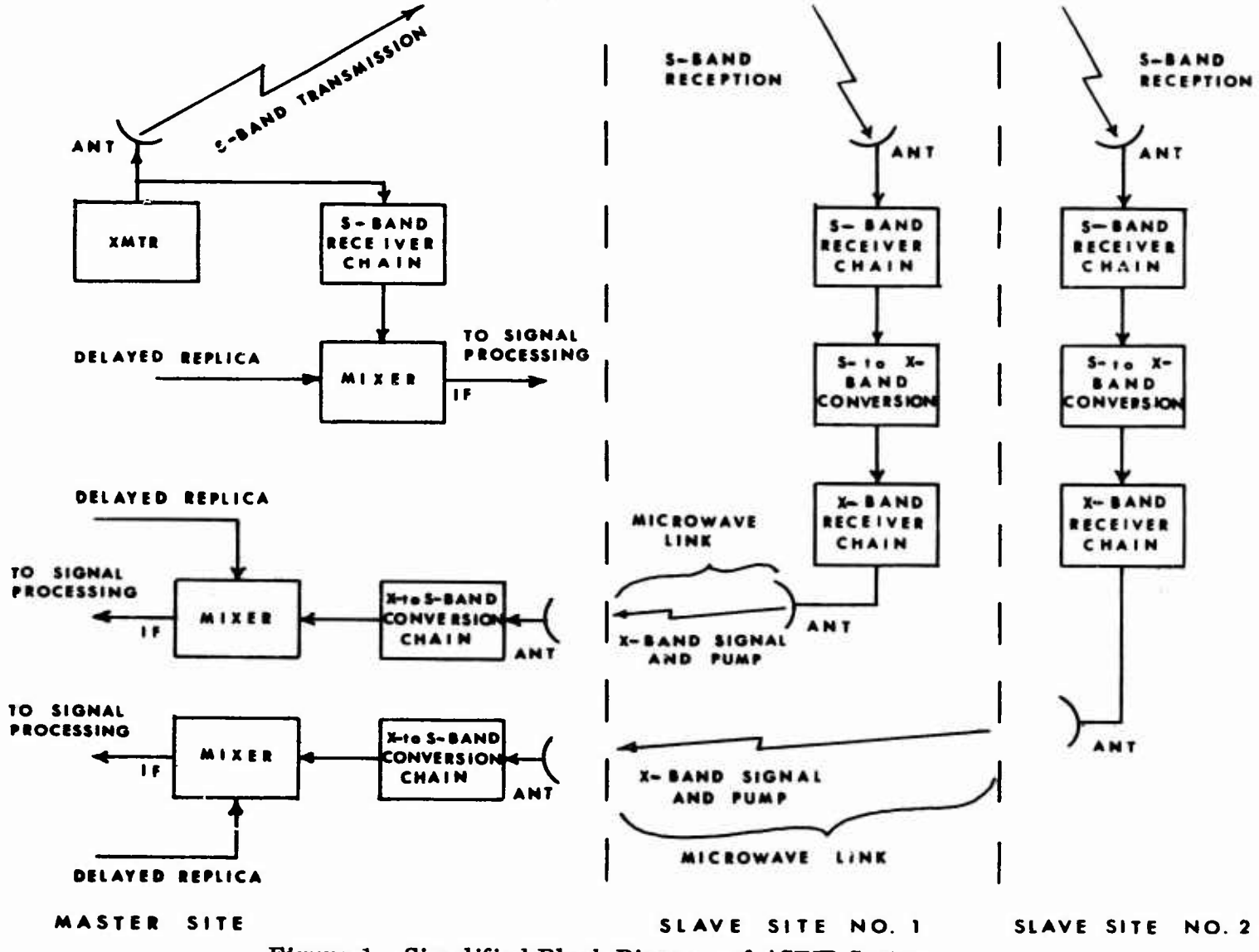

Figure 1. Simplified Block Diagram of ASFIR System

The following reference analyzes the quantitative effects of specific phase distortion functions on radar resolution.[2] In general, phase distortion is manifested by a shifting, widening, and/or asymmetry of the main spectral lobe. Side lobe levels may increase and additional lobes are likely to appear, giving rise to spurious "targets."

If the time of transmission of a sinusoidal signal through a network is τ, then the phase angle in radians through which the signal will rotate during that time is given by

$$\phi = \omega\tau \tag{1}$$

If τ is to be constant over a frequency band, then the phase shift of the network must be linear with frequency over that band. It is the departure from linearity of this characteristic that results in what is known as phase distortion. If now the transmission of a group or packet of signals is considered, such as occurs with a train of periodic pulses, then, provided that τ is constant with frequency, the signals will arrive at the receiver after a time, τ, with their relative phase relations preserved. However, if τ is not constant, then distortion of the envelope will result and its exact time of arrival becomes difficult to define. An early analysis of a problem similar to the one under discussion[3] has shown that envelope transmission time is closely related to the slope of the network's phase shift characteristics. It has become conventional then to describe the phase delay as

$$\tau_P = \frac{\phi}{\omega} \tag{2}$$

and the envelope or group delay as

$$\tau_E = \frac{d\phi}{d\omega} = \tau_P + \omega \frac{d\tau_P}{d\omega} \tag{3}$$

It can be seen that the envelope delay is equal to the phase delay, plus a term which accounts for the variation in phase delay with frequency.[4]

The phase vs. frequency characteristics measured in this report are deviations from linear phase over the signal frequency band. The envelope delay of the device under test was measured and a very nearly linear reference delay line was inserted in the reference branch to equalize reference and test branch delays. This procedure increased the measurement accuracy tremendously since now the measured quantity varied only a few degrees across the signal frequency band. If the envelope delay had been measured directly, and deviations in envelope delay measured across the signal frequency band, the error would have been much greater, since the quantity measured would have been many thousands of degrees in magnitude. Fine grain data would have been impossible to achieve.

Active devices in the ASFIR system had rigid amplitude and phase linearity specifications. Amplitude variations across the signal frequency band were limited to $\pm.5$ db maximum variation and the phase linearity specification was $\pm.36^{\circ}$/MHz.

There are many methods for measuring phase. It is not the intent of this report to investigate various phase measurement techniques. Rather, several methods that were used for the measurements of this report will be discussed.

SECTION III

PHASE MEASUREMENT METHODS USED

A. General Phase Comparison Method

A fairly general method of measuring phase distortion is given in Figure 2. This method is commonly referred to as the phase comparison method. A signal from the microwave source is split (by means of a directional coupler, magic tee, etc.) into a reference and test signal.

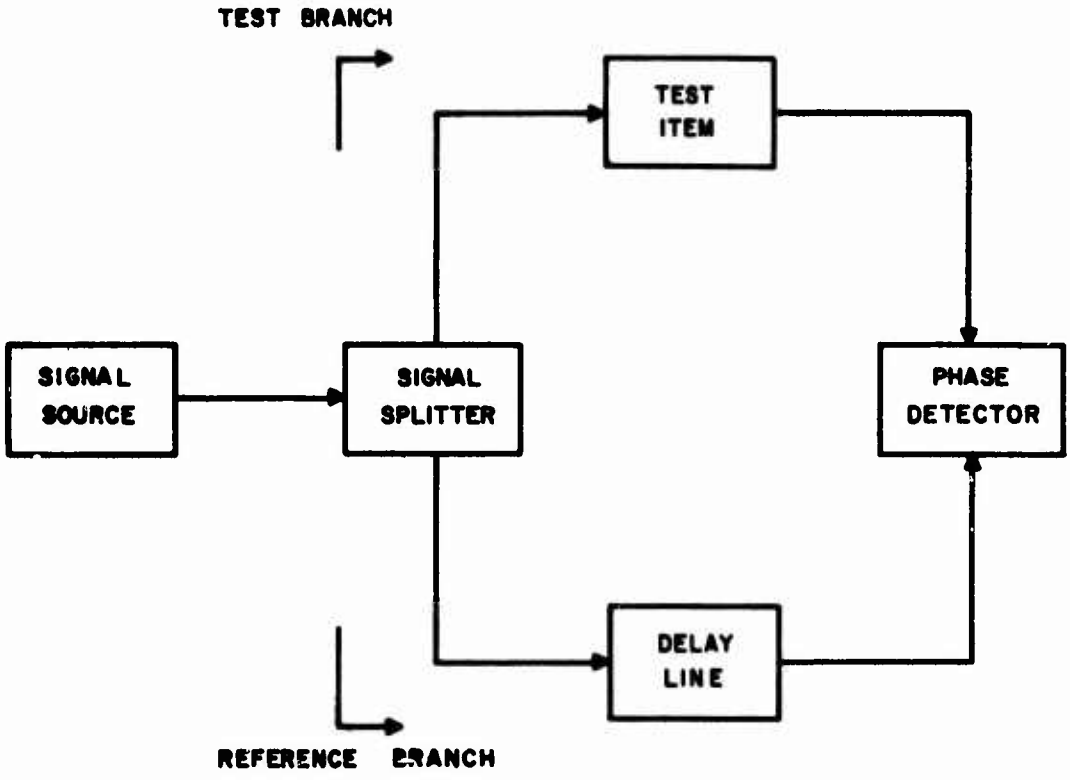

Figure 2. General Phase Comparison Method

The test signal is sent through the test item (unknown) and is recombined with the delayed reference signal in the phase detector. The phase detector compares the reference signal and the test signal, and provides an output phase reading.

The two methods used for the phase measurements of this report both are phase comparison methods. They differ mainly in their approach.

A phase measurement system using a double probe slotted-line detector is given next. This system was used during the preliminary investigation covered in this report. The phase indicator and phase detector used for these measurements were among the first commercially available.

B. Double-Probe Slotted-Line Detector

1. Pulsed Measurements

Two different operations may be used in making phase measurement using the arrangement of Figure 3. Both reference and test branches may be pulsed or one input may be CW and the other pulsed.

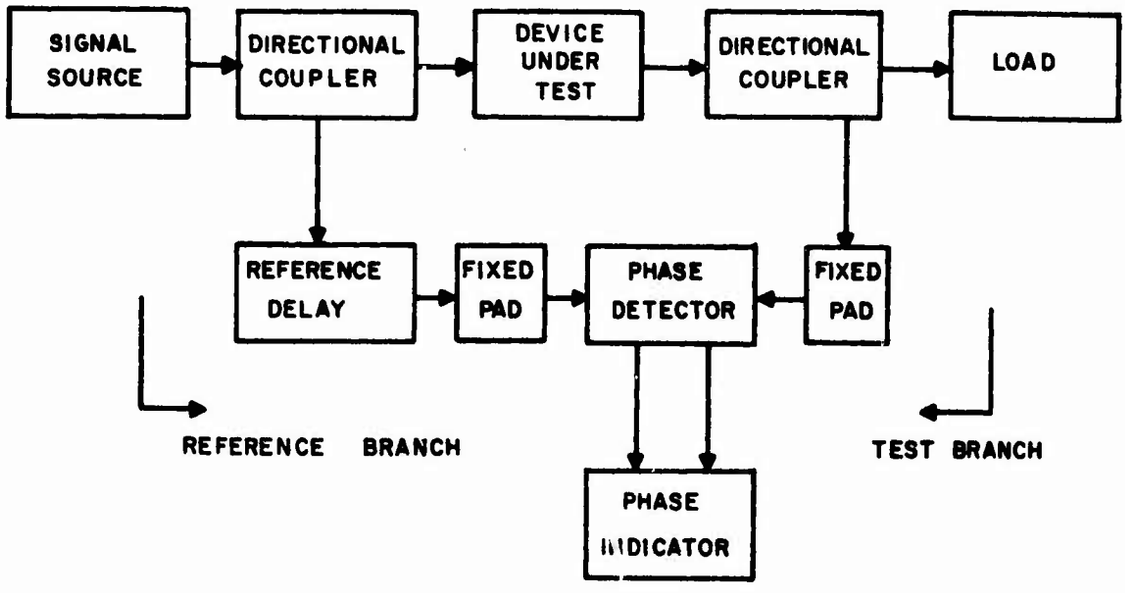

Figure 3. Typical Circuit Arrangement for Slotted-Line Phase Measurement

Phase is measured by sampling the standing-wave pattern in the slotted line. The pattern position is indicative of the relative phase of the two signals sent into the slotted line. Phase may be read directly on a meter or by a position readout. For the phase measurements of this report, phase was measured by a position readout. In the case of phase measurements by a position readout, the two detector probes on the slotted line are positioned to straddle a null so that the phase meter (indicator) is used as a very sensitive null detector. At each new phase reading, the double probe detector is moved to the tracked null position where the meter reads zero. The phase change is proportionate to the linear position of the detectors. Phase changes are recorded by distance measurements above the line. If L is a measured change of detector position on the slotted line in centimeters, phase shift in degrees is computed by the following formula:

$$\text{Phase shift in degrees} = \frac{(L)\ (360^{o})\ (2)}{\lambda}$$

where λ is the wavelength in centimeters. Phase measurements are made directly. There is no intermediate step of phase shifting one signal and null seeking.[5]

In determining the phase linearity (phase vs. frequency) characteristics of a device using the above method, phase samples are taken at a number of fixed frequencies across the signal frequency band. A detailed analysis and formulas for computing phase linearity are presented in another paper written by the author.[6]

An error analysis of this measurement system is presented in the next section of this report.

2. Error Analysis

To obtain a good phase measurement system, certain precautions are necessary. Suitable power levels must be supplied to the phase detector, the signal source must have little incidental FM, frequency harmonics should be kept 30 or 40 db below the energy signal content, a low pass filter should be used if harmonics are present, and the signal source should have good frequency stability.[7] In addition, the attenuators next to the slotted line must be matched, unwanted reflections kept to a minimum, phase measurement system components should have low VSWR's, the directional couplers must have high directivity, waveguide flanges should be carefully mated, and coaxial cable connections should be tight without undue flexing of the cable. All of these precautions and more are necessary to obtain an effective phase measurement system.

The phase linearity specification on individual components of the ASFIR system was $\pm .36^{o}$/MHz. Since phase measurements were made every 5 MHz, another way of stating the above is that the maximum deviation of phase from linear could not be greater than $\pm 1.8^{o}$ over any 5 MHz frequency range. It is conceivable that a test device could have a sharp resonance or phase discontinuity that could fall between test points. This phenomenon would be readily apparent using a swept-frequency technique of measuring phase. It would have been possible to use a servo adapter unit on this particular phase measurement system to provide automatic null tracking on a

swept-frequency basis, but the calibrated phase shifter portion of the servo adapter unit alone had a phase accuracy of $\pm .5^{o}$. Servo drive backlash, additional reflections in the bridge circuit, and residual phase curvature in the branches would also contribute to phase error, using a servo adapter unit. Other methods of obtaining accurate phase data on a swept-frequency basis were investigated, and the measurement scheme listed in Section III (C) of this report, appeared to be very promising. If this new measurement system had not been available, the servo adapter unit would likely have been obtained for further measurements using the double probe slotted-line phase detector since certain system phase deviations can be taken out of swept-frequency phase data by a system calibration procedure. This is pointed out in the following reference. [8]

In order to obtain an idea of the errors involved in a phase measurement system, it is good practice to make an analysis of phase errors. The claimed accuracy of several manufacturers of phase measurement equipment in the period 1963-1964 (purchase time of the phase measurement equipment used for measurements of this report) was typically $\pm 1^{o}$. To measure phase deviations of $\pm 1.8^{o}$, phase measurement accuracy should be an order of magnitude better, i.e., $\pm .18^{o}$. There was no phase measurement system then available with this accuracy, so steps were taken to improve the measurement accuracy of the systems available.

The accuracy claims of the manufacturer are as follows: (1) Phase differences of $.25^{o}$ are resolved; (2) overall accuracy depends on reflection errors in getting signal to point of measurement, on input VSWR to phase detector which is specified for each model, and on indicator meter error of 2% full scale range being used; (3) noise fluctuation less than 1^{o}, peak-to-peak; and (4) phase shift due to reflections from detector system less than $.3^{o}$. [9] Note that accuracy is dependent upon the phase indicator (meter) range and is 2% of the full scale range being used. For this reason, the lowest range scale was used and the reference branch time delay was made approximately equal to the test branch time delay. By making the test and reference branches electrically equal, deviations from linear phase response are obtained when measurements are taken over the desired frequency range. In addition, large changes in phase between frequency points are eliminated. Large phase changes can mask small perturbations. If undesirable FM is present on the signal source, the result will be phase fluctuations on the phase indicator if reference branch and test branch delays are unequal.

The component tolerances of a phase measurement system are very rigid. Certain uncertainties exist in phase measurements due to unavoidable mismatch of circuit components in the reference and test branches. Reflections alter the relative phase of the oppositely traveling wavefronts in the slotted line. An analysis of reflection errors is given next. The following symbols are used in the analysis and are defined below:

Symbol	Definition
E_1	Signal entering the slotted line by way of the reference branch.
E_2	Signal entering the slotted line by way of the test branch.

γ_1	Composite reflection coefficient from the E_1 direction.
γ_{in}	Reflection coefficient at input of device under test.
γ_{out}	Reflection coefficient at output of device under test.
D	Directivity (ratio of coupled reverse signal to coupled forward signal).
γ_L	Reflection coefficient of load.
β	Phase constant.
L	Slotted line axial length.
γ_2	Composite reflection coefficient from the E_2 direction.

A signal flow graph solution of the slotted line[10] provides the following equations. The total signal from the reference branch is:

$$\frac{E_1 + E_2\ \gamma_1 \ell^{i\beta L}}{1 - \gamma_1 \gamma_2 \ell^{i2\beta L}} \tag{5}$$

The total signal from the test branch is:

$$\frac{E_2 + E_1 \gamma_2 \ell^{i\beta L}}{1 - \gamma_1 \gamma_2 \ell^{i2\beta L}} \tag{6}$$

The maximum phase errors are:

$$\mathrm{Sin}^{-1}\ \frac{E_2 \gamma_1}{E_1} \tag{7}$$

$$\mathrm{Sin}^{-1}\ \frac{E_1 \gamma_2}{E_2} \tag{8}$$

The above equations are useful for several reasons. Equations 7 and 8 show the errors involved when E_1 and E_2 are of varying magnitudes, and equations 5 and 6 will be useful in analyzing reflection interactions discussed in the next section. The

previous reference also gives formulas for the leading contributors to phase error. The equation for maximum phase angle error in E_1 is:

$$\text{Sin}^{-1} \quad (\gamma_{in} D) \tag{9}$$

The equation for maximum phase angle error in E_2 is:

$$\text{Sin}^{-1} \quad (\gamma_L D + \gamma_L \gamma_{out}) \tag{10}$$

A sample computation will give an indication of what maximum errors can be involved. Let D = 34 db, $\gamma_{in} = \gamma_{out} = .2$, $\gamma_1 = \gamma_2 = .05$, $\gamma_L = .025$ and $E_1 = E_2$.

The maximum error in phase angle of E_1 from equation (9) is:

$$\text{Sin}^{-1} \quad (.2 \times .02) = .2^{o} \tag{11}$$

The maximum error in phase angle of E_2 given by equation (10) is:

$$\text{Sin}^{-1} \quad (.025 \times .02 + .025 \times .2) = .3^{o} \tag{12}$$

Maximum reflection interaction error occurs when equations (7) and (8) are additive. In this case the maximum error is:

$$\text{Sin}^{-1} \frac{E_2}{E_1} \gamma_1 + \text{Sin}^{-1} \frac{E_1}{E_2} \gamma_2 =$$

$$\text{Sin}^{-1} .05 + \text{Sin}^{-1} .05 = 2.87^{o} + 2.87^{o} = 5.74^{o} \tag{13}$$

Equation 13 shows that if E_2 is much larger than E_1, the error becomes very large and no reading is possible. This is one reason why E_1 and E_2 should be approximately equal. Another reason for keeping E_1 and E_2 essentially the same amplitude is so that standing wave pattern minima (nulls) will be relatively well defined.

Convenient nomograms for finding the maximum possible phase error introduced by a two-part network and from paired discontinuities is given in the following reference.[11] The author points out that maximum phase errors of ±1 degree can exist for identical 1.02/1 mismatches at the slotted line ends.

A detailed analysis of all phase errors is too lengthy to be included in this report. Instead, values will be given for certain additional phase errors. The slotted-line probe outputs are square law detectors and a phase uncertainty exists due to detector unbalance. This error is approximately ±.6 degrees if $E_1 = E_2$ assuming a .2 db detector sensitivity unbalance. If $E_1 = 10E_2$ (-20db), this uncertainty is approximately

±3 degrees. Probe reflection error can become much greater than ±.3 degrees stated by the manufacturer if $E_1 = 10E_2$.

From the previous error analysis, it is seen that maximum phase uncertainties can be slightly greater than ±7 degrees. The probability that the subject errors would be correlated, or add in their worst phases, is extremely remote. Instead, a rms error criterion has been proposed for phase deviations that can be categorized as "random."[12]

In summary, it is apparent from the subject error analysis that many precautions are necessary to achieve a good phase measurement system. Reflections cause the most serious errors in phase measurement. In the worst case, phase errors can be slightly greater than ±7°. For the best case, phase errors would cancel and there would be zero error.

3. Effectiveness of Phase Measurement System

Phase data taken manually using the slotted-line detector is very time consuming. It required almost an hour to sample the phase at eleven fixed frequency points. Many man hours were required to set up the phase measurement system. It was necessary to measure the VSWR of all system components to insure that these components were not introducing excessive phase errors into the system.

In a phase measurement system which contains waveguide, it is desirable to cancel the dispersive effects of the waveguide in the test branch. This can be done by placing waveguide of similar dispersive characteristics in the reference branch.

Many manhours are often required in plumbing waveguide to equalize the time delay and dispersive characteristics of the reference and test branches.

Phase measurements taken on the phase measurement system itself showed that maximum phase departure from linearity was typically ±1 degree over a 50 MHz frequency range.

The effectiveness of the phase measurement system decreased when the phase characteristics of certain active devices are measured. A drifting of the tracked null with time was experienced. This drift introduced an error into the phase data, giving erroneous results and non-repeatable data. A technique for minimizing this error was devised and is given in the following report.[13]

The need for swept frequency phase measurements of high accuracy was apparent. The particular type of phase measurement equipment used for swept frequency measurements will now be described.

C. Phase-Discriminator and Detector

The phase measurement system that will be described next has the following desirable features: Phase angle in degrees is directly readable on a meter, recorder, and oscilloscope; accurate phase data is available on a swept-frequency basis without point-by-point adjustments being necessary; phase readings are not adversely affected

by the attenuation or gain of the component under test or by the output power of the signal source: sensitivity is sufficient for the test of low-noise preamplifiers, such as, masers, parametric amplifiers, and tunnel-diode amplifiers; calibration is simple and stable, and phase readings have sufficient resolution to indicate phase differences of .1 degree[14].

An especially attractive feature of this phase measurement system is that the complete system is provided by the manufacturer. The complete system has been engineered to minimize all sources of phase error. In addition, experience has shown that the required reference delay line length is very easily calculated from the phase vs. swept frequency output display presentation.

1. CW and CW Swept Frequency Measurements

A simplified block diagram of the phase measurement system which uses a phase-discriminator and detector is given in Figure 4. The input CW or CW swept frequency signal, is divided by a hybrid tee into a reference and a test signal. The test signal is modulated by a 1000-cps balanced modulator, passes through the item being tested, and then is recombined with the delayed reference signal in a phase-discriminator circuit. The phase-discriminator circuit (referred to as phase-discriminator and detector in this report) phases the reference and test signals in such a way that the output of one detector is proportional to sin θ, where θ is the phase difference to be measured, while the output of the other detector is proportional to cos θ. The phase indicator is a ratio-computing device that yields tan θ, which is the ratio of the two detector outputs. [15]

If phase linearity is the desired measurement, the phase vs. frequency slope (time delay) of the reference branch is made approximately equal to that of the test branch. This is accomplished by inserting coaxial cable (which has very nearly linear phase vs. frequency characteristics) in the reference branch. Fine phase slope adjustments are accomplished by means of a line stretcher in the reference branch. Phase vs. frequency or phase vs. another parameter can be measured using CW swept frequency or CW frequency operation respectively.

This system requires only minor changes for pulsed signals. Pulsed phase measurements will be discussed next.

2. Pulsed Measurements

There are two principal situations in measuring pulsed signals. Either the system can be operated with a pulsed signal in the test branch and a CW carrier in the reference branch, or with pulsed signals in both branches. The balanced modulator shown in Figure 4 is biased into a constant transmission state for pulsed measurements. The only modifications required in the system for pulsed measurements are removal of all or most of the padding in the test branch, and connection of the detector outputs to a pulse adapter unit, and thence to the phase indicator.

For pulsed operation, phase vs. time during the pulse can be measured at fixed frequencies, and phase vs. frequency can be measured when the frequency varies during the pulse.

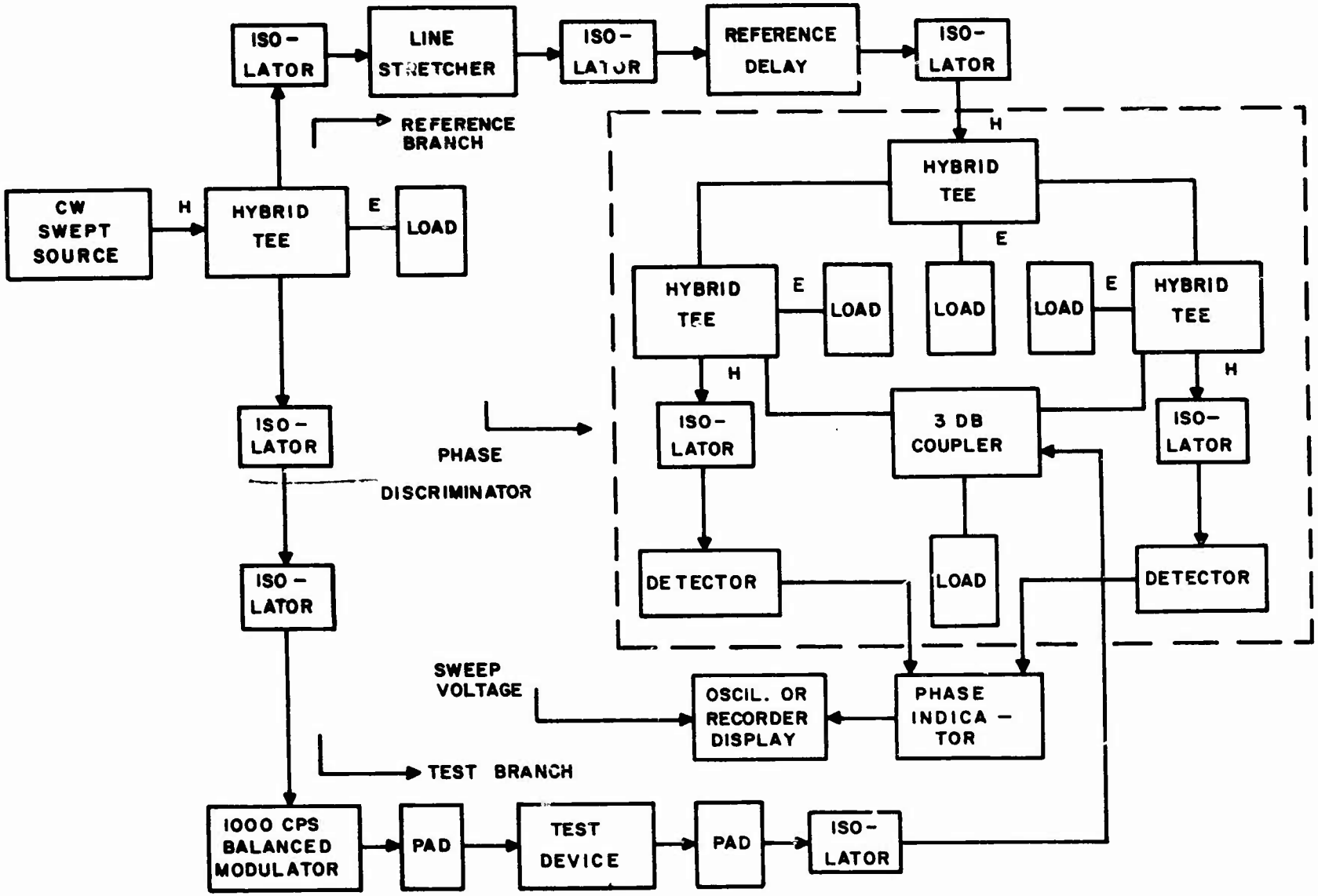

Figure 4. Simplified Block Diagram of Phase Measurement System Using Phase-Distriminator and Detector

Factors contributing to phase errors in this system will now be discussed.

3. Error Analysis

It was mentioned in Section III-2, of this report, that certain phase errors can be taken out of the phase data by a calibration procedure. This calibration procedure was used for the measurements of this report.

An error analysis of this measurement system is given in the following reference.[16] The authors list two types of error: (1) Randon reading errors due to noise, and (2) systematic errors due to imperfections of the system and its components. Noise error is given as a maximum of $.05^{o}$ peak-to-peak. Meter scale error is determined by mathematical law and is held to less than $.25^{o}$. Linearity of detection error is negligible. The maximum angular error due to amplitude unbalance in the phase discriminator and detectors is $.65^{o}$. Phase error due to improper phase relations at the detectors is a maximum of $.5^{o}$ due to all causes. Phase error resulting from undesired carrier in the balanced modulator branch is less than $.2^{o}$. Leakage signals in the phase-discriminator will result in a phase error less than $.2^{o}$. Leakage of modulated signal through the reference branch and of CW signal into the test branch can cause a phase error of $.2^{o}$ maximum. Several additional errors arise when swept frequency measurements are made. Reflection interaction errors yield a maximum uncertainty of $\pm 1.36^{o}$. Uncompensated phase curvature also adds to interaction phase shifts. A total system phase non-linearity of about ±1 degree results over the entire operating frequency band.

Accuracy of pulsed test signal and CW reference signal operation is essentially the same as with CW signals, except for an error due to non-suppressed carrier. This error is bounded by $\pm .3^{o}$ for the typical case. If both reference and test signals are pulsed, additional error exists due to detector unbalance, and deviation from square law.

It should be noted that the test device can contribute to reflection interaction error, if the mismatch at the input and output parts of the test device is appreciable. Human error in reading values from the output presentation is also a factor in any measurement system.

Phase curvature and interaction error may be eliminated from phase vs. swept frequency measurements by a calibration process presented in Section II-B-1 of this report. These errors are the most important errors in the measurement system, and since they can be taken out by a calibration process, the overall phase error is reduced considerably.

It was mentioned previously in this report that it is extremely unlikely that all phase errors will be maximum and in phase at the same time.

For the measurements of this report the maximum error was approximately $\pm .5^{o}$. This accuracy was obtained by the following method:

- Phase curvature and interaction errors were eliminated from phase vs. swept frequency data by a calibration process.
- Reference delay cables were lossy low VSWR cables to minimize reflection interactions.
- The measurements performed were deviations from linearity and not the total phase shift of the device under test. Consequently, the measured readings were small (usually less than 10 degrees) and accuracy was improved.
- A highly sensitive X-Y recorder was used for phase vs. frequency display. This recorder indicated phase differences of better than $.1^{o}$.
- The phase measurement system was supplied power from a regulated power source to minimize phase fluctuations due to line voltage changes.
- Phase vs. frequency readings were taken only over the 50 MHz frequency band of interest and not the 2.65-3.25 GHz range of the S-band phase measurement system.

In summary, it is apparent from the above error considerations that many sources of error exist in a phase measurement system of this type, but many of these errors can be eliminated. Reflection interaction and phase curvature errors can be eliminated from the system by a system calibration process.

4. Effectiveness of Measurement System

Phase measurements taken with this system were fast and had good accuracy. The time required to sample over a 50 MHz frequency range is typically several seconds. Phase is read directly on an output display, and no intermediate step of mathematical calculations is necessary. A real time, or essentially real time, readout of phase permitted fast and convenient observation of the effects of changing test device parameters. Amplitude levels in the test branch could vary somewhat without adversely affecting system performance or system error.

In the interest of brevity the foregoing describes rather superficially the method of phase measurement which is much more elaborately discussed in reference 14. It is suggested that at this point the reader obtain a copy of the February 1964 Microwave Journal and review the article by S.B. Cohn and N. P. Weinhouse prior to continuing into Section IV.

SECTION IV

PHASE MEASUREMENTS PERFORMED AND TEST RESULTS

A. Tests Performed Using Double-Probe Slotted-Line Detector

Initial phase testing was initiated in November 1963. Essentially all investigations utilizing the preliminary phase measurement method were completed in March 1964, although some tests were performed in August 1964. Tests were performed at S- and X-bands. S-band tests were performed at 5 MHz frequency increments from 2.975 GHz to 3.025 GHz. X-band tests were performed at 5 MHz frequency increments from 9.975 GHz to 10.025 GHz. The X-band system was waveguide throughout, including the slotted line; whereas, the S-band system was coaxial throughout, including the slotted line.

1. Calibration

There are two types of calibration to be considered for this phase measurement system, i.e., equipment calibration and a calibration test run. Equipment calibration consisted mainly in calibrating the phase meter at each frequency point (procedure is given in reference 5) and calibrating the positional indicator dial. The position indicator dial indicated position differences of .0001 cm. Calibration against a standard showed that the dial indicator had a maximum error of ±.0003 cm over its maximum travel distance of 5 cm. At 10 GHz, λg is approximately 4 centimeters and the error involved with position readout is approximately ±.05°. At 3 GHz, λ is approximately 10 centimeters and the position readout error is a maximum of ±.02°.

A typical calibration run is shown in Figure 5. Run 1 is a phase vs. frequency measurement on the phase measurement system itself. Waveguide was used throughout the system. Variation across the band is a maximum of +.85° and -.35°. There is normally some phase slope in the phase vs. frequency data due to unequal time delays in the reference and test branches, but this slope has been taken out mathematically for most runs in this report. Run 1 showed that the error introduced by the phase measurement system was not as large as might be anticipated. It should be noted, however, that the many precautions listed in the error analysis section of this report had to be taken to achieve these results. In addition, it was necessary to regulate the line voltage of the phase measurement system. The test data shown in this report represents only a small fraction of the data taken.

2. Coaxial Cable and Waveguide

Figure 6 shows a test run on coaxial cable. Since the phase measurement system was waveguide (small x), it was necessary to use two waveguide-to-coaxial adapters for the test. Run 2 shows the effects on phase of two adapters and a coaxial cable. The maximum deviation from linearity for this test is +.7° and -.55° or a total of 1.25° peak-to-peak across the frequency band. Deviation from linearity

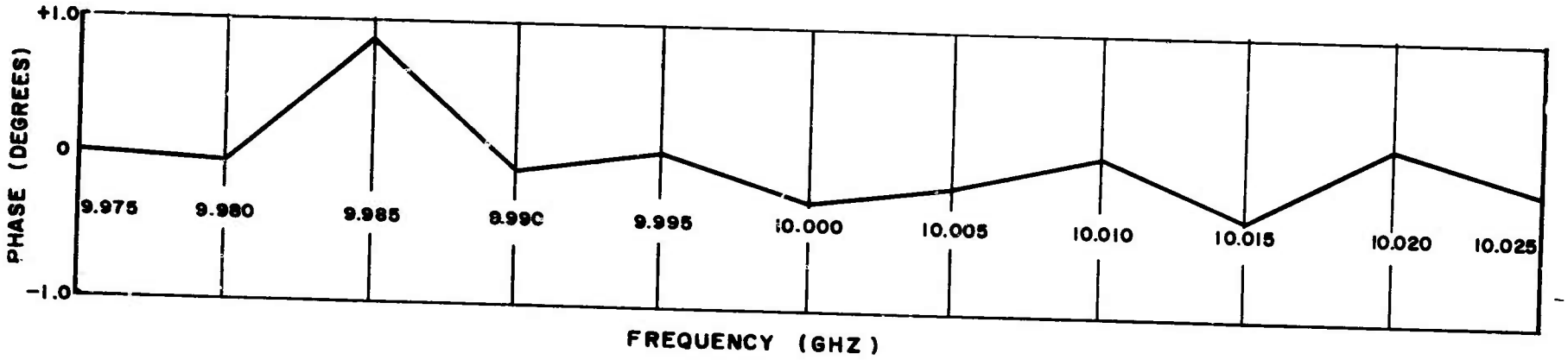

Figure 5. Calibration Run on Waveguide Phase Measurement Set-up. Run 1. 15 November 1963. VKG.

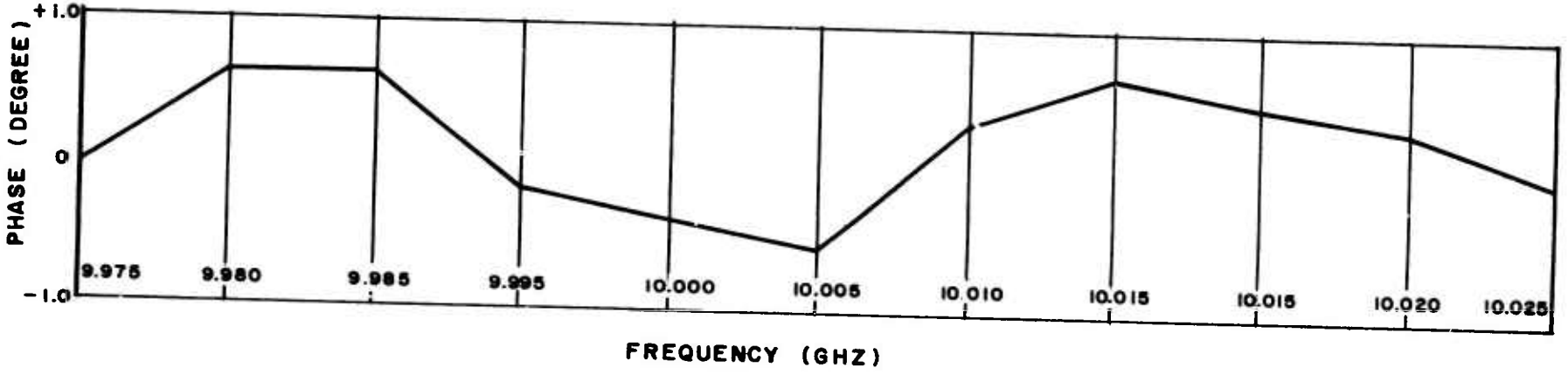

Figure 6. Calibration Run on Waveguide Phase Measurement Set-up with 3 ft. Coaxial Cable as Test Device. Run 2. 3 December 1963. VKG.

exceeds that of the phase measurement system alone, which is understandable, and most of the deviations in excess of system deviations can be attributed to reflections at the waveguide-to-coaxial adapters. Future tests on coaxial cable indicated that coaxial cable has very nearly linear phase vs. frequency response.

The following reference[17] states that the form of the time delay characteristics obtained for waveguide and transmission lines indicates that signal distortion is not a problem of line discontinuity but one of line termination. This is indicated by the ripple of the envelope delay characteristics correlating directly with the transmission line theory which relates VSWR to delay variation.

Although coaxial cable has very nearly linear phase vs. frequency characteristics (constant time delay), this does not imply that it is absolutely linear. Most manufacturers of phase measurement equipment use coaxial cable as reference delay, but it had not been accepted as a "phase" standard at the time of the tests conducted in this report. In referring to coaxial cable as having very nearly linear phase vs. frequency characteristics, it is assumed, of course, that connectors have such low VSWR that their contributions to phase deviations are negligible.

It is well known that waveguides, in particular waveguides operating near their cutoff frequencies, are dispersive devices.[18]

3. Traveling-Wave Tube Amplifiers

The phase vs. frequency characteristics of two waveguide-to-coaxial adapters, two coaxial cables, and a traveling-wave tube amplifier in cascade are shown in Figure 7. Comparison of Run 3 with Runs 1 and 2 shows that the maximum phase deviation of cascaded devices becomes greater as more devices are cascaded. Part of the phase perturbations can be attributed to non-linearity of the traveling-wave tube amplifier, and the rest is attributed to additional reflections among the cascaded test pieces, phase instability of the traveling-wave tube amplifier, and phase measurement equipment errors. Maximum phase deviations were $+.8^{o}$ and -1.8^{o} or a total of 2.6^{o} peak-to-peak.

Runs 4 and 5 were repeated runs made on a series connection of three coaxial cables, two waveguide-to-coaxial adapters, a waveguide variable attenuator, and two traveling-wave tube amplifiers. The phase deviations for both runs were huge compared to those of the phase measurement system alone or of the single traveling-wave tube amplifier measured in Run 3. Note that the deviations for the two runs are somewhat similar in nature, but the phase vs. frequency characteristics are not repeatable. The sampled phase differed by as much as 3.6 degrees at corresponding frequency points. Maximum phase non-linearity for Run 4 was $+8.1^{o}$ and -3.4^{o}, and for Run 5 maximum deviation was $+10.6^{o}$ and -2.2^{o}. Phase deviations were much more than expected from individual test component contributions, and data was not repeatable. At this time, further investigation was begun to determine the cause, or causes of the excess phase deviation and lack of repeatability.

The manufacturer of the traveling-wave tube amplifiers had considered the following chief contributors to phase deviations: (1) variations in cold circuit phase velocity from one portion of the helix to another; (2) reflections produced by imperfections or impedance discontinuities along the helix; (3) input drive level; and

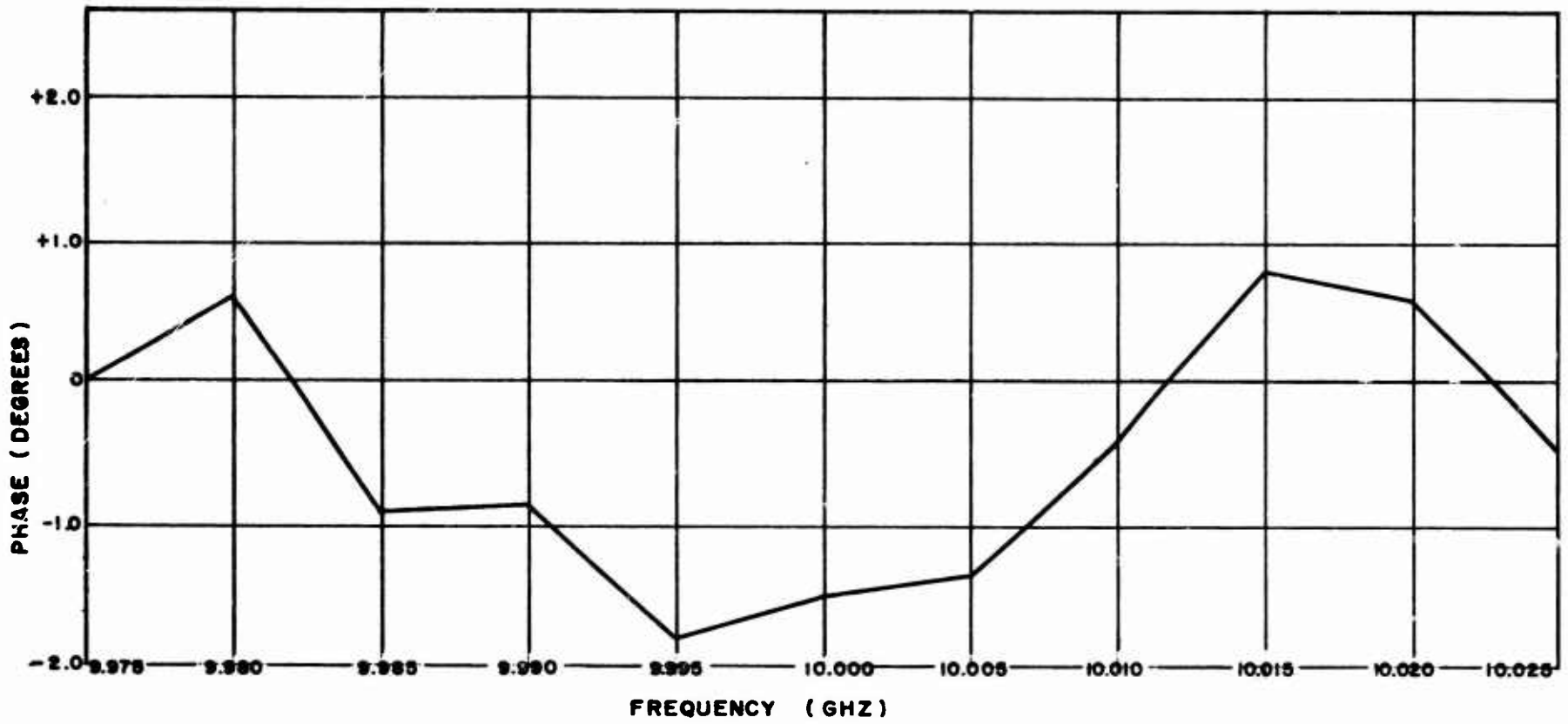

Figure 7. Phase vs. Frequency Characteristics of Two Coaxial Cables and Traveling-Wave Tube Amplifier in Cascade. Run 3. 5 December 1963. VKG.

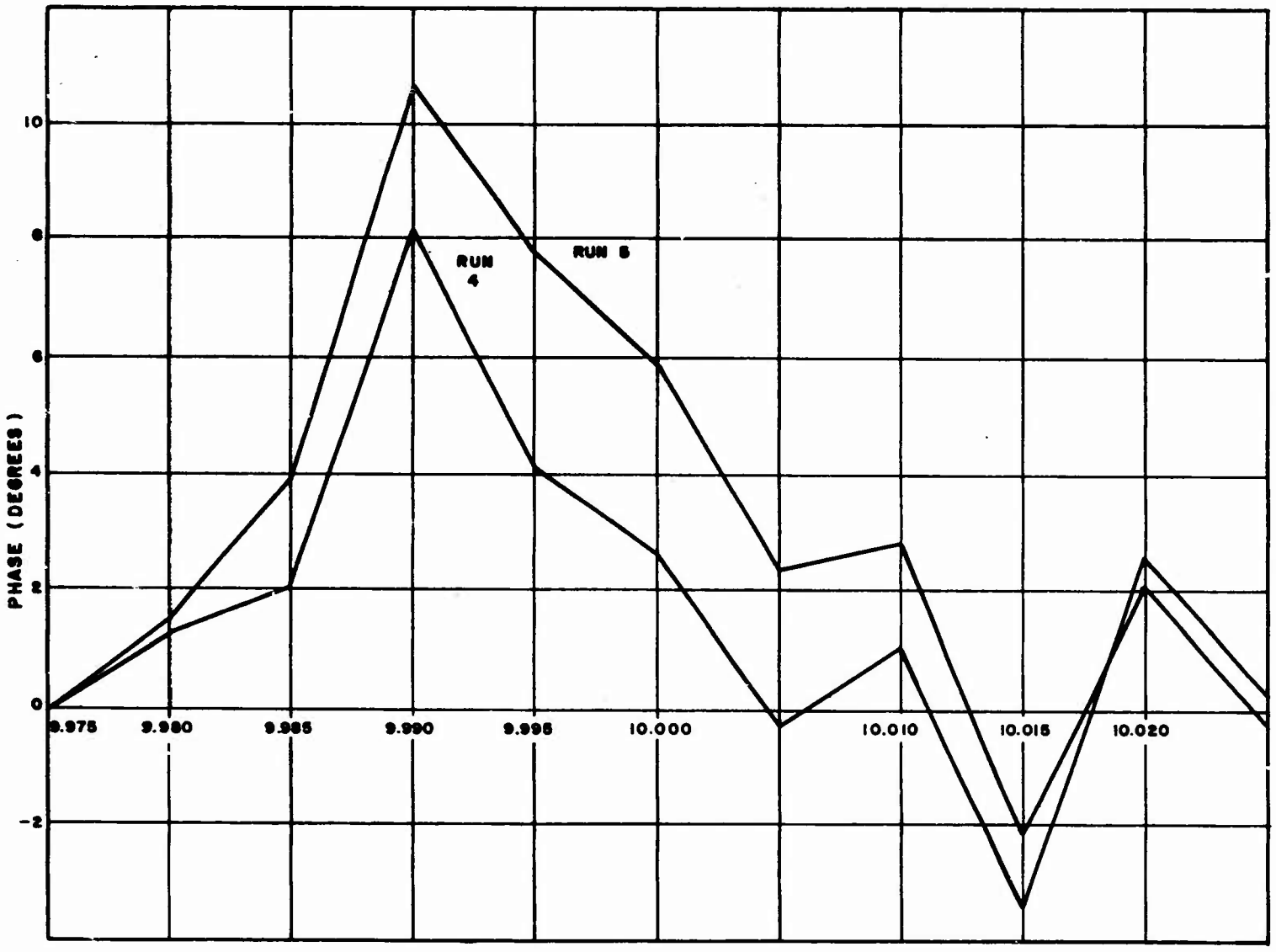

Figure 8. Phase vs. Frequency Characteristics of Cascaded Test Devices. Three Coaxial Cables and Two Traveling Wave-Tube Amplifiers. Repeated Runs. 17 January 1964. Runs 4 and 5. VKG.

(4) power supply fluctuations.[19] Contributions of (3) and (4) were not difficult to measure, and these were the first areas of investigation. Input drive level phase deviations occur when the input r-f drive level approaches that required to saturate the traveling-wave amplifier. The electrical length of the tube changes due to a change in effective beam velocity. Power supply phase deviations are minimized by careful power supply design. Phase sensitivity with respect to helix voltage is the most critical power supply deviation. All critical voltages on the traveling-wave tube were regulated to provide phase stability.

Run 6 of Figure 9 shows incremental phase shift vs. power input drive level of a traveling-wave tube amplifier. As the input r-f drive level approaches that required to saturate the traveling-wave tube amplifier, phase changes due to input drive become greater. If the input drive level fluctuates, undesirable phase shifts occur. The significance of this to the system engineer is that traveling-wave tube amplifiers should be operated at input power levels at least 15 db below input saturation, to minimize phase shifts due to changes in input drive power. In making fixed frequency phase measurements, power input drive to traveling-wave amplifiers should be held constant for each fixed frequency measurement. It should be noted that the phase shift plot of Figure 9 has a small phase error due to the waveguide variable attenuators used to vary power input. The power inputs from the reference and test branches into the slotted line were maintained at equal levels to minimize phase errors. This was mentioned previously in the error analysis section.

The next area of investigation was the phase sensitivity with respect to helix voltage of the traveling-wave tube amplifiers. Voltages were measured with a differential voltmeter to obtain high accuracy. By varying the helix voltage and recording the shift in null position, it was experimentally determined that one low noise X-band traveling-wave tube amplifier had a phase sensitivity of 12^{o}/volt when tested 15 db below saturation at a frequency of 10 GHz. The phase sensitivity of a medium power X-band TWT (traveling-wave tube amplifier) was 2.8^{o}/volt while that of another low noise X-band TWT was 10.4^{o}/volt. Helix voltages of the various TWT's were monitored using a differential voltmeter to observe voltage fluctuations. This was done in order to provide an indication of the magnitude of phase stability error resulting from helix voltage fluctuations. Observed changes of helix voltage were $\pm.04$ volts for the low noise TWT's and $\pm.2$ volts for the medium power TWT. Helix voltage fluctuations can result in phase stability errors of $\pm.48^{o}$ and $\pm.42^{o}$ for the low noise TWT's and a phase stability error of $\pm.56^{o}$ for the medium power TWT. In the worst case, when the errors are additive, phase instability error can be as much as $\pm1.46^{o}$. The rms error due to phase instability is $\pm.85^{o}$.

Figure 10 shows repeated runs on three traveling-wave tube amplifiers, five coaxial cables, two multiplexers, a waveguide variable attenuator, and two waveguide-to-coaxial adapters in cascade. Even though many precautions were taken, such as regulating all line voltages, maintaining a constant power level at least 15 db below input saturation to the TWT's, etc., the runs show that the phase measurements are not repeatable. Since the data is not repeatable, the question of what the phase linearity of the test devices actually is remains in doubt. The difference in sampled phase at a given fixed frequency differs by as much as 10 degrees.

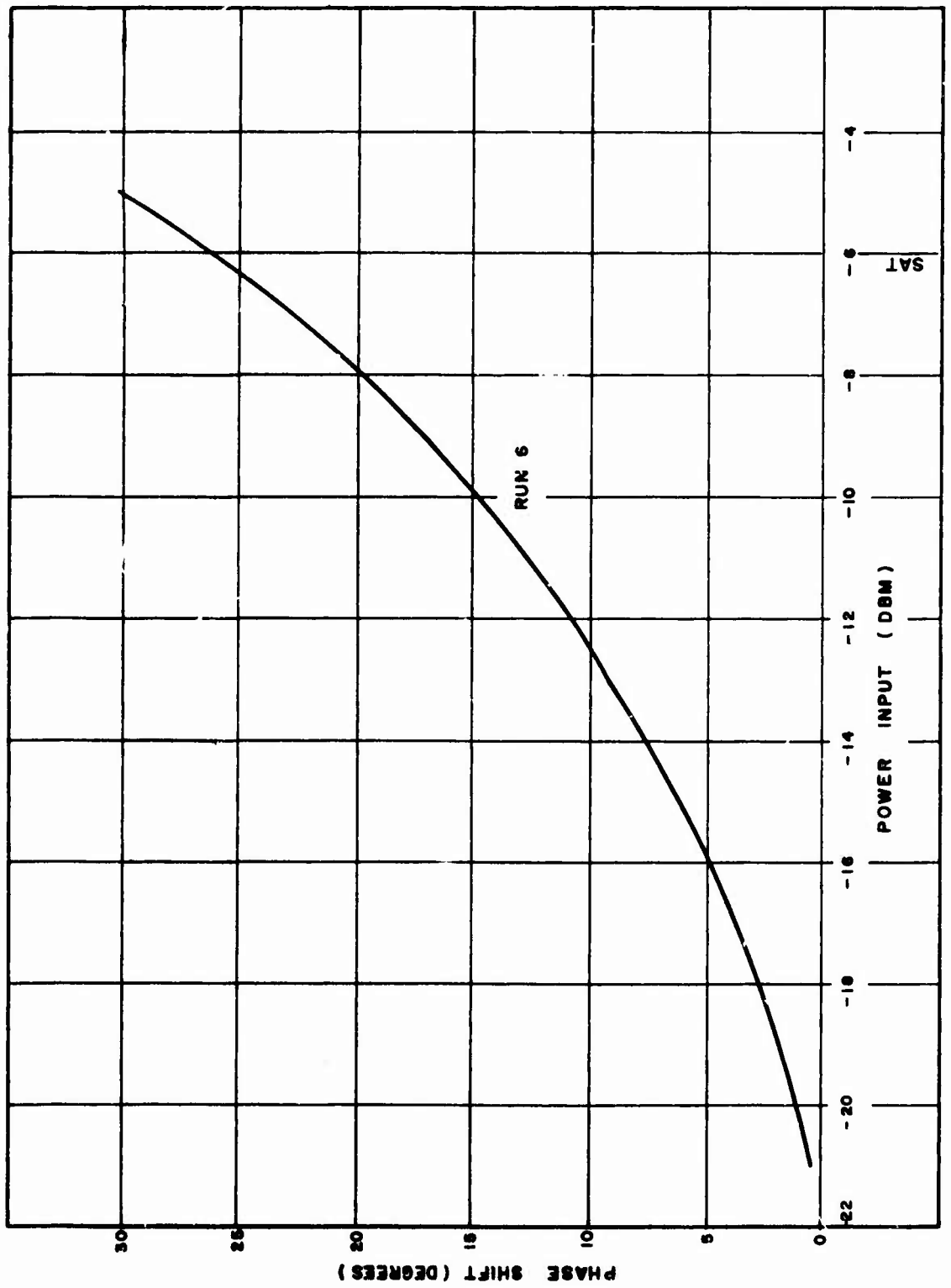

Figure 9. Incremental Phase Shift vs. Power Input Drive of Traveling-Wave Tube Amplifier. Run 6. 20 February 1964 (Frequency of 9.98 GHz, Saturation Occurring at -6 DBM Power Input). VKG.

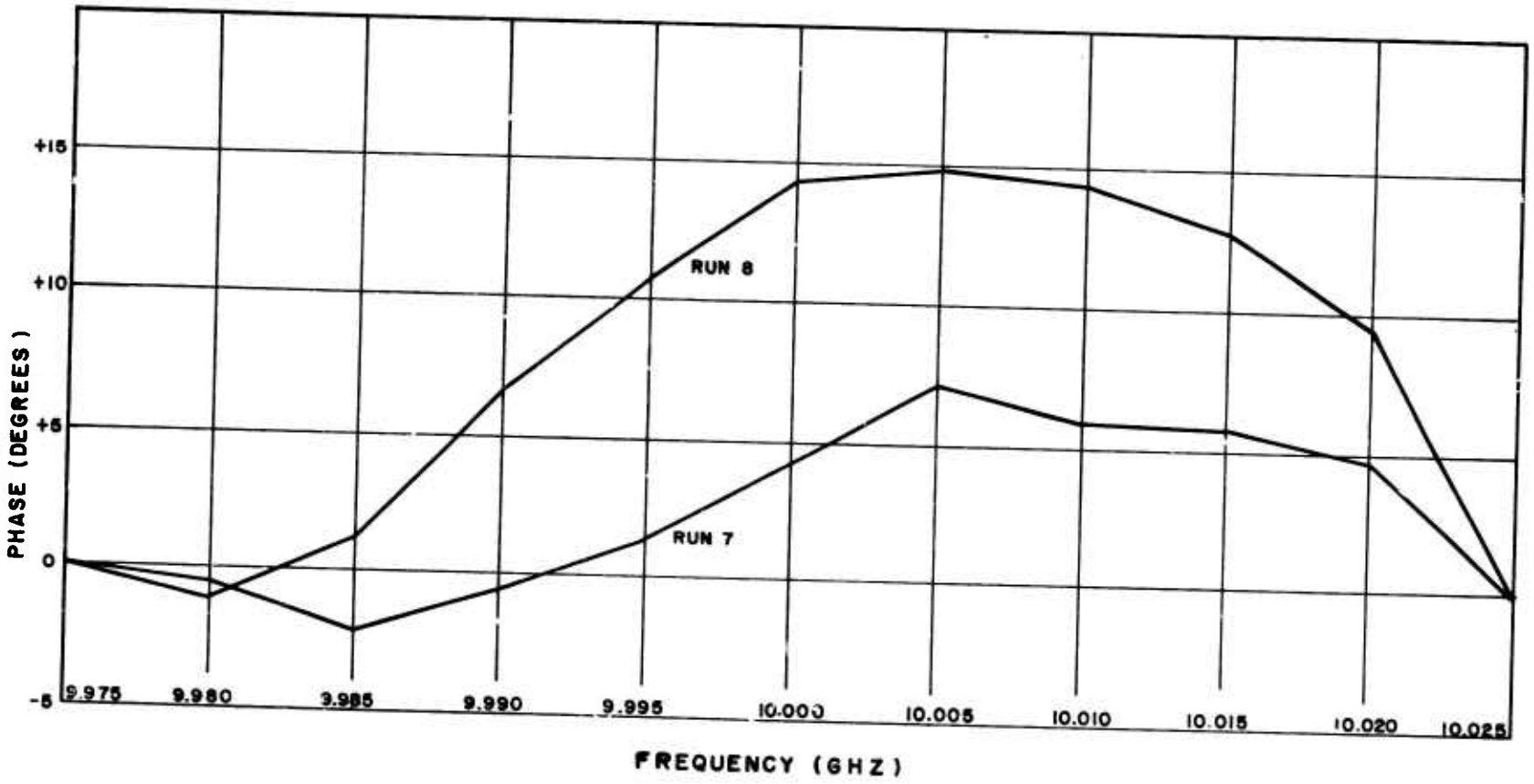

Figure 10. Phase vs. Frequency Characteristics of Three Traveling-Wave Amplifiers, 5 Coaxial Cables, 2 Multiplexers, Waveguide Variable Attenuator and 2 Waveguide-to-Coaxial Adapters. Repeated Runs. 26 February 1964. Run 7 and 8. VKG.

It was becoming more and more apparent that there were other factors involved in obtaining good phase data. Investigation now turned to measuring possible drifting of the tracked null with time. A plot of null shift with time is shown in Figure 11. Since the time between any two fixed frequency phase samples was approximately four minutes, drifting of the null position with time would introduce error into the phase data. Run 9 shows the drift in null position over an eight minute time interval of the phase measurement system itself. It is seen that there is some drift and at the end of eight minutes, the null has drifted .35°. This drift is somewhat constant with time and would introduce a small error into the phase data. Run 10 shows the corresponding drift in null position over an eight-minute time interval for the items tested in Runs 7 and 8. This drift can cause serious phase errors. The error due to drifting of the null was +5.7° at the end of four minutes, and -7.4° at the end of eight minutes.

Run 11 of Figure 12 shows the effect of changes in environmental room temperature upon a reference null. Temperature was maintained constant to within ±1°F. Note the effect of the air conditioning unit. When the air conditioning unit was on, and temperature was decreasing, the null always drifted in the same direction. When the air conditioning unit was off, the null always drifted in the opposite direction. Changes in temperature can change the electrical lengths of the reference and test branches, since thermal expansion and contraction of long waveguide runs will change the electrical lengths. The phase meter also was temperature sensitive. This resulted in a drift of the zero and balance settings with time.

Runs 10 and 11 showed that if fine grain repeatable data was desired, environmental temperature must be maintained fairly constant, and drifting of the tracked null must be monitored. An air conditioning/heating unit maintained temperature to within ±1°F and drifting of the reference null was monitored by using an additional frequency source. Details of this technique are given in another report by the author.[20] This method will subsequently be referred to as the two-source method.

Phase vs. frequency data was again taken on the test items of Runs 7 and 8. Runs 12 and 13 are repeated runs on these items. Data was taken using the two source method and the elapsed time between reference null and data null readings was from 30 to 40 seconds. The results now show much better correlation between runs, and phase error due to a drifting null has been reduced by a factor of four in the worst case.

Repeated tests using the two-source method showed that phase uncertainties due to all causes was ±1.5° maximum for the test items of Runs 7 and 8. Runs 12 and 13 showed that the phase non-linearity of the components under test was within acceptable limits. This concluded this particular series of tests.

In summary, phase linearity measurements at fixed frequency points across a desired frequency band are time consuming and inaccurate. When the test device consists of two or more cascaded TWT's plus certain interconnecting passive components, obtaining accurate and repeatable phase data becomes extremely difficult. To achieve reasonably good results, such precautions as maintaining constant input power drive level to the TWT's, operating the TWT's at least 15 db below input saturation, regulating all line voltages, maintaining fairly constant environmental temperature, etc., are necessary. To minimize the effects of a drifting null some method such as

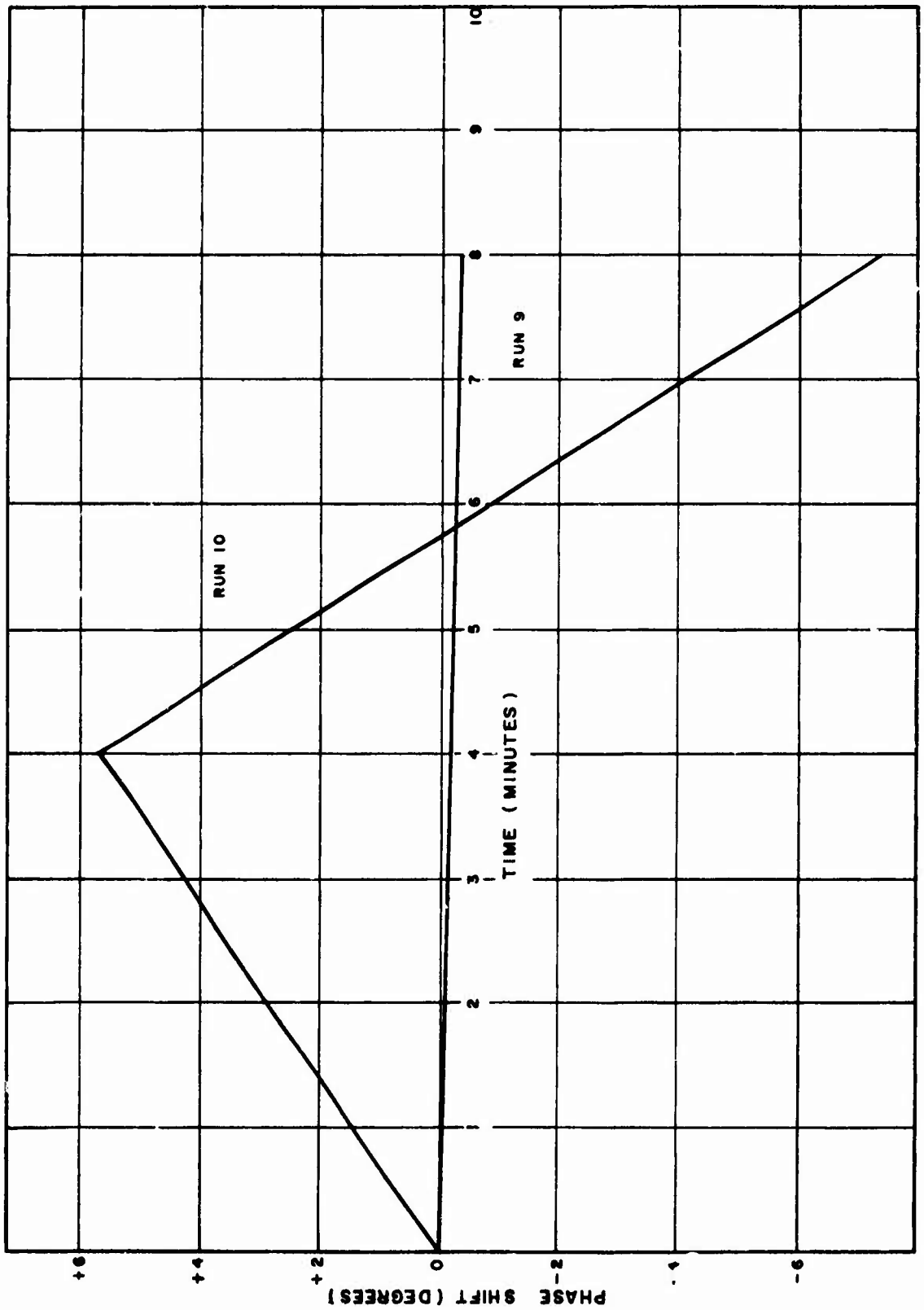

Figure 11. Phase Shift vs. Time (Freq = 9.975 GHz). Run 9 Shows Drift of Tracked Null With Time for Phase Measurement System Alone. Run 10 Shows the Drift for the Items Tested in Runs 7 and 8. VKG.

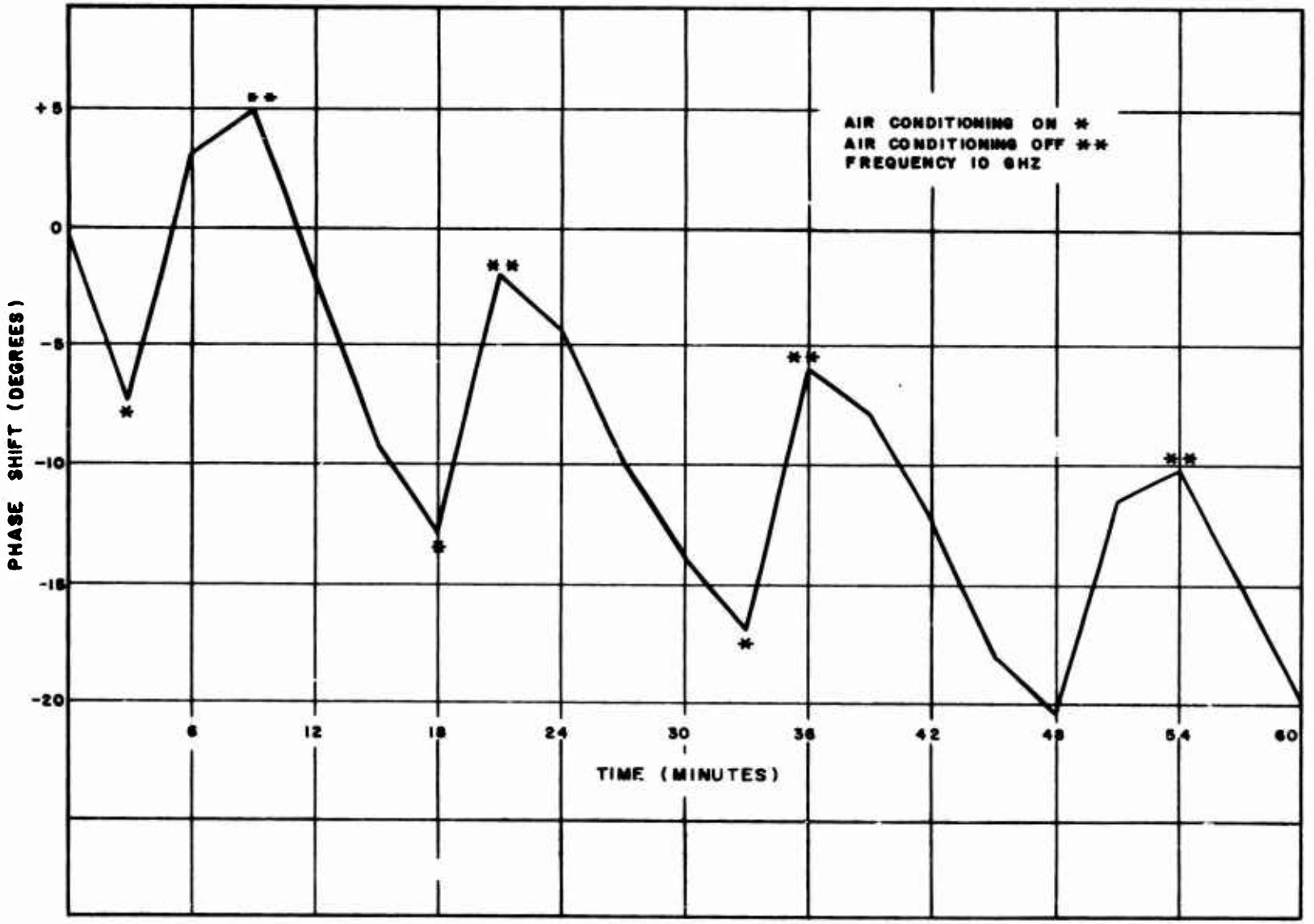

Figure 12. Phase Shift vs. Time. Run 11 Shows the Effect of Environmental Room Temperature Changes Upon Drifting of the Reference Null. Temperature Maintained Within Less Than 2^{o}. Items Tested are Those of Runs 7 & 8. 3 March 1964, Run 11. VKG.

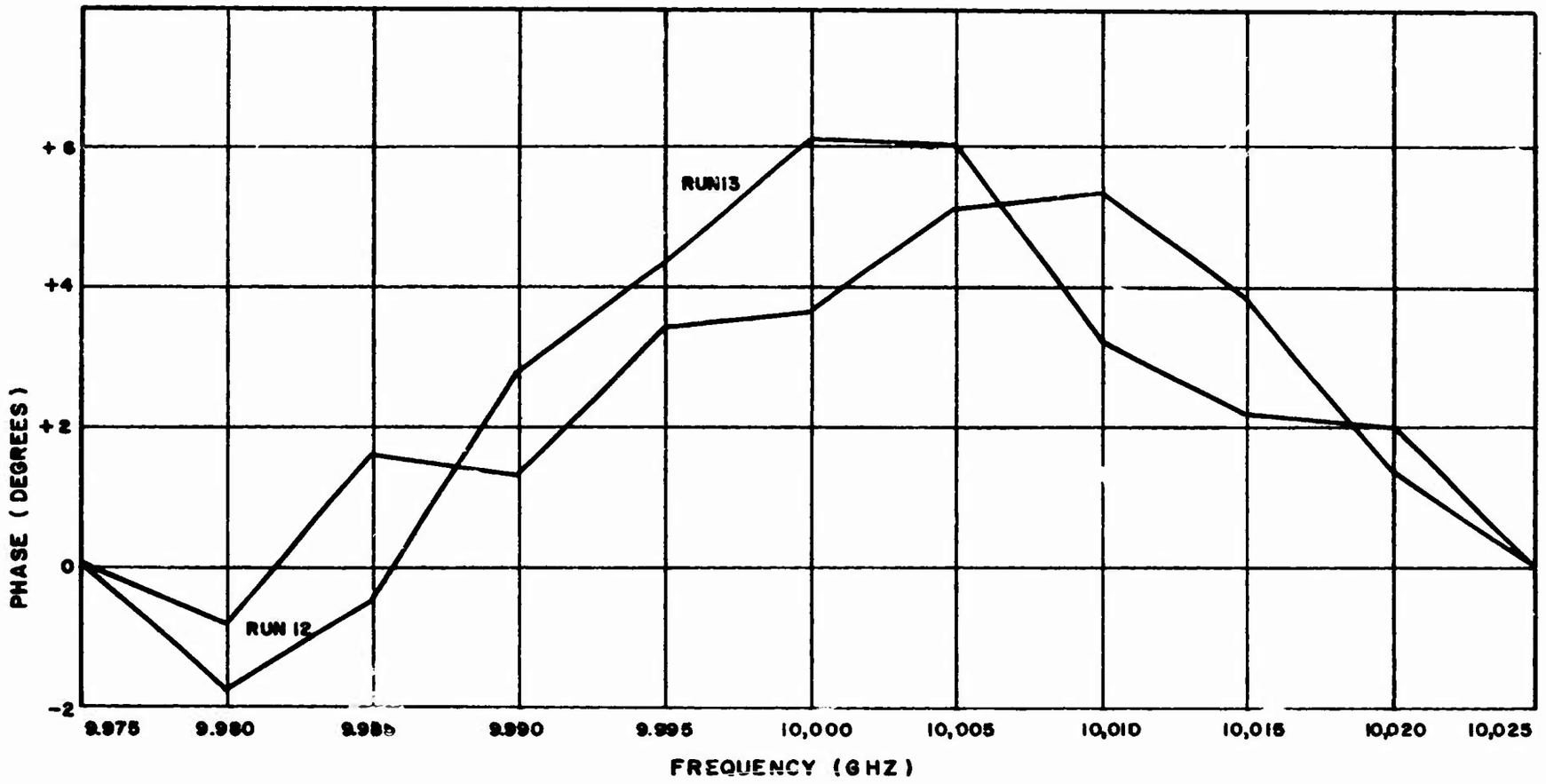

Figure 13. Phase vs. Frequency Characteristics of Test Items of Runs 7 and 8. Test Made by Two-Frequency Source Method. 19 March 1964. Runs 12 and 13. VKG.

the two-source method is required. These are only some of the more important precautions that are necessary in phase linearity testing of a group of cascaded devices at fixed frequencies.

4. Transmitter

Phase linearity tests on the ASFIR transmitter were performed at S-band using a coaxial slotted line detector. Phase was sampled at 5.0 MHz frequency increments from 2.975 to 3.025 GHz. The reference branch operated CW and the test branch operated pulsed. Figure 14 shows a block diagram of the r-f portion of the transmitter.

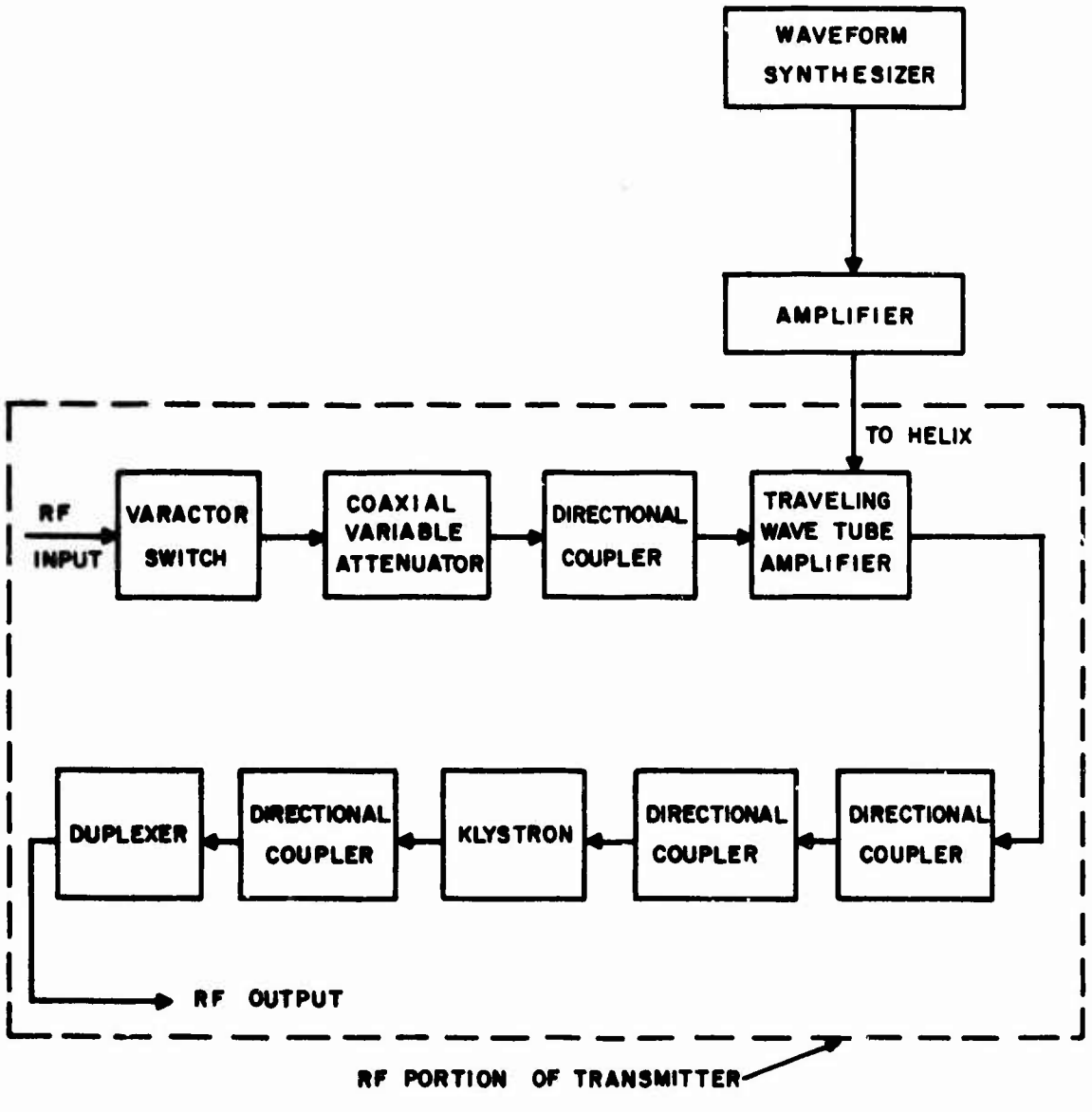

Figure 14. Block Diagram of RF Portion of Transmitter

The transmitter is essentially built around the high power klystron. This klystron has seven cavities and operates at 50 KW average power. A traveling-wave tube amplifier is used to provide input drive to the klystron. The traveling-wave tube amplifier has been modified to permit phase corrections to be applied to the helix. Phase correction is accomplished by means of a waveform synthesizer. The waveform synthesizer applies a programmed video output of adjustable slope and amplitude to the TWT helix to correct phase non-linearities of the transmitter.

Line voltage fluctuations were causing unwanted phase instability in the klystron when measuring phase at fixed frequencies. An adjustable power supply was connected in series with the klystron body to maintain a constant voltage throughout the runs.

To correct phase non-linearities at fixed frequency readings, the first frequency position on the slotted line is used. If this reference null does not drift, the procedure is simply to correct subsequent frequency slotted-line positions to the reference slotted-line null position. This is done by means of the waveform synthesizer. It should be emphasized that the amplitude and slope of the voltage waveform between test points must be an assumed value. There is no way of knowing exactly what it should be unless measurements are taken on a swept frequency basis. If the reference null drifts with time, which it did, then a technique such as the two-source method must be used. The two-source method was used for all transmitter and klystron phase testing at fixed frequencies to improve accuracy.

Figure 15 shows a plot of phase vs. frequency taken on the transmitter. Phase non-linearity was as great as 26 degrees across the frequency band. Run 15 of Figure 16 shows the phase vs. frequency characteristics of the transmitter after phase correction using the waveform synthesizer. The phase non-linearity is now a maximum of 2.25 degrees.

Run 16 of Figure 17 is the phase vs. frequency characteristics of the klystron itself. It is seen that a large percentage of phase deviation of the overall transmitter is due to the klystron. Block diagrams of the various test set-ups are contained in another phase measurement report.[21]

B. Tests Performed Using Phase Discriminator and Detector

A swept frequency phase measurement system was obtained in May 1964, and all future phase measurements were made with this unit. Tests were performed at S-band since this is the operating band of the radar. The slave sites up-convert the S-band received signals to X-band and transmit the up-converted signals and local oscillator signals across a microwave link to the master site. At the master site, the X-band signals and local oscillator signals are mixed and the original S-band signals received at the slave sites are obtained. Since the phase measurement system cannot operate at both S- and X-band frequencies simultaneously, all phase measurements were performed at S-band.

1. Calibration

Calibration is obtained in two parts. The first part consists of a series of self-calibration procedures for calibrating the phase measurement system. The second part consists of a swept-frequency phase measurement of the phase measurement system itself. With the test terminals of the phase measurement system

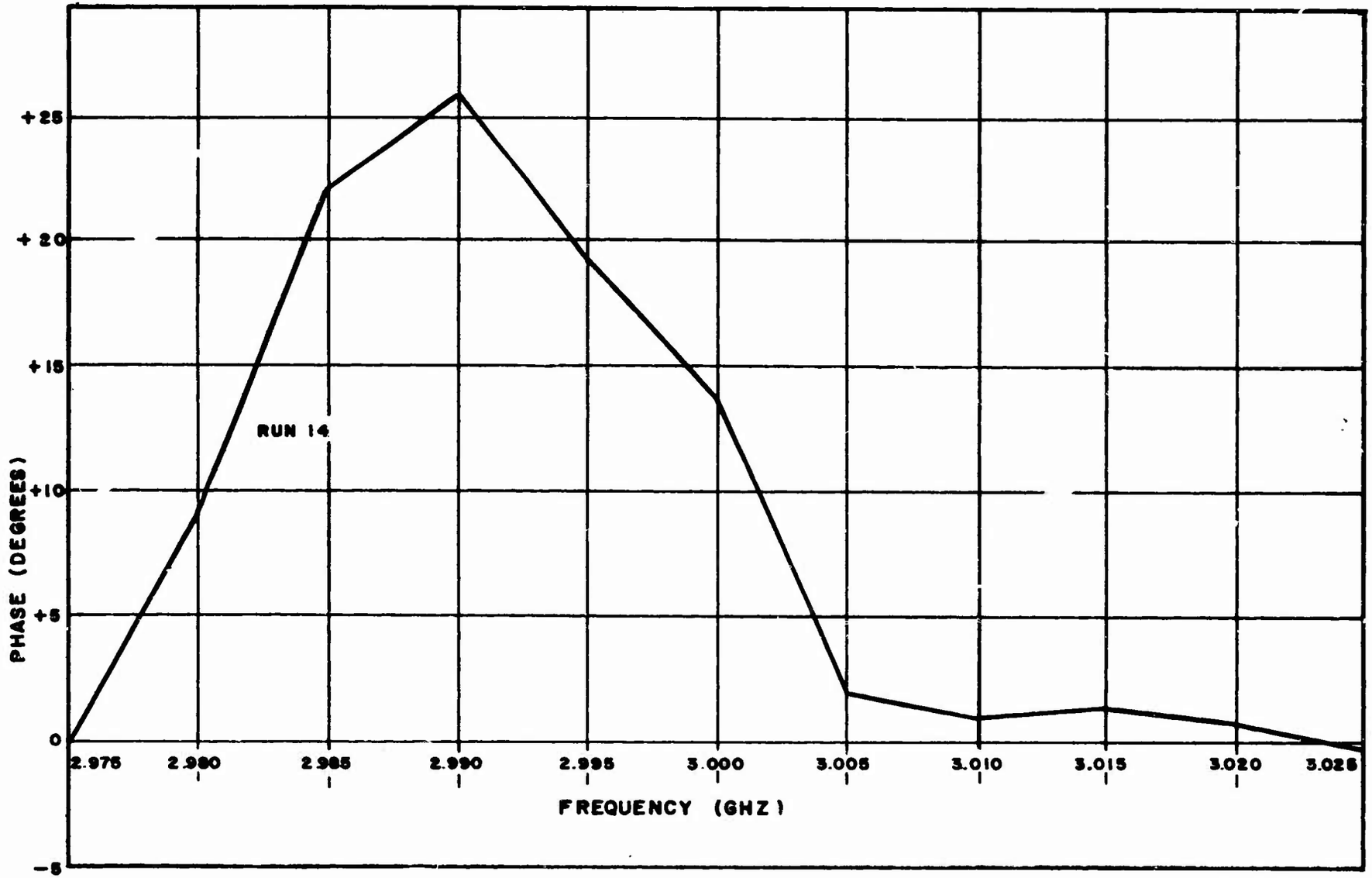

Figure 15. Phase vs. Frequency Characteristics of Overall Transmitter. Two Source Method. 22 August 1964, Run 14. VKG.

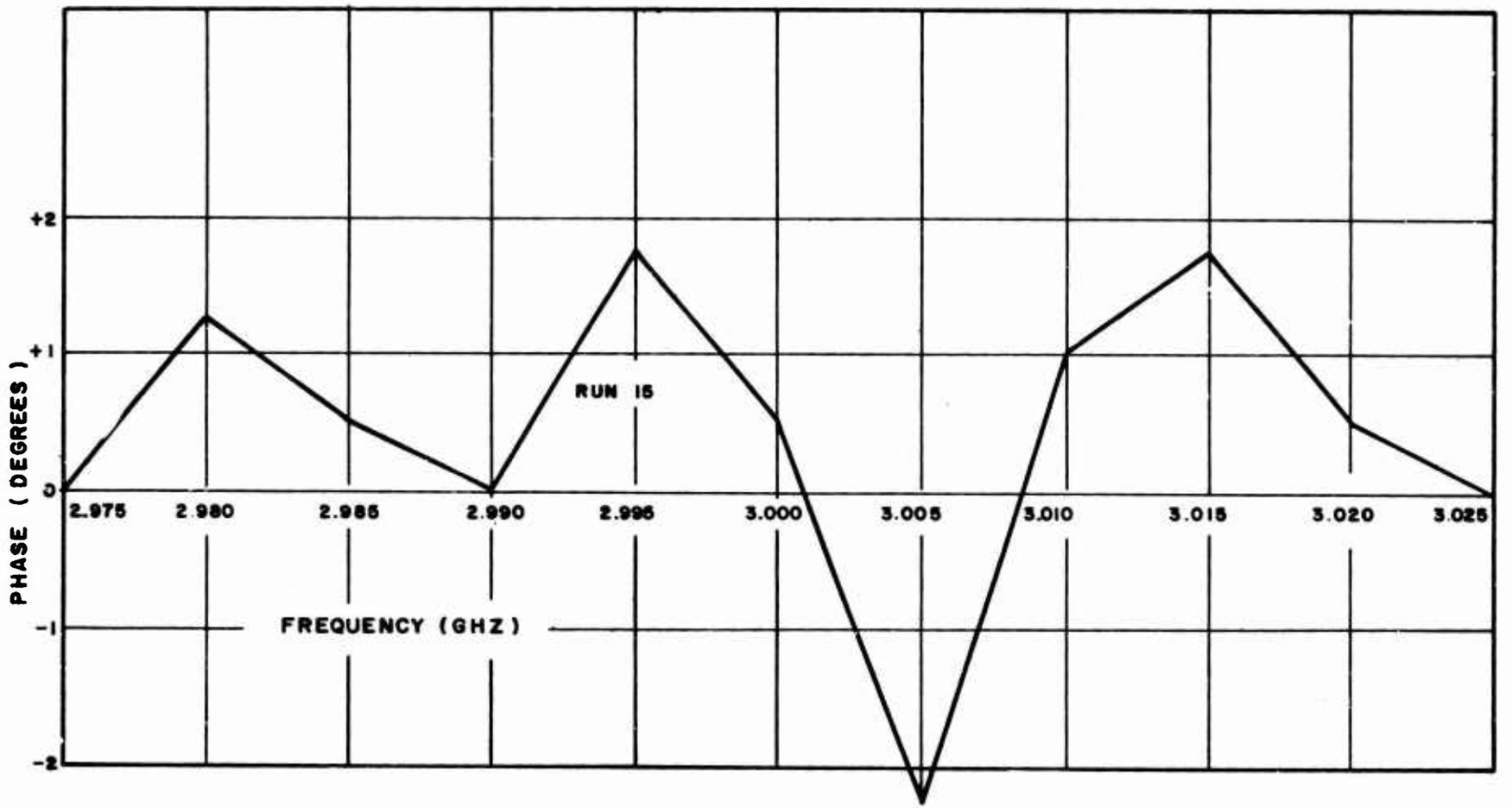

Figure 16. Phase vs. Frequency Characteristics of Overall Transmitter After Being "Phase Corrected." Two Source Method. 25 August 1964, Run 15. VKG.

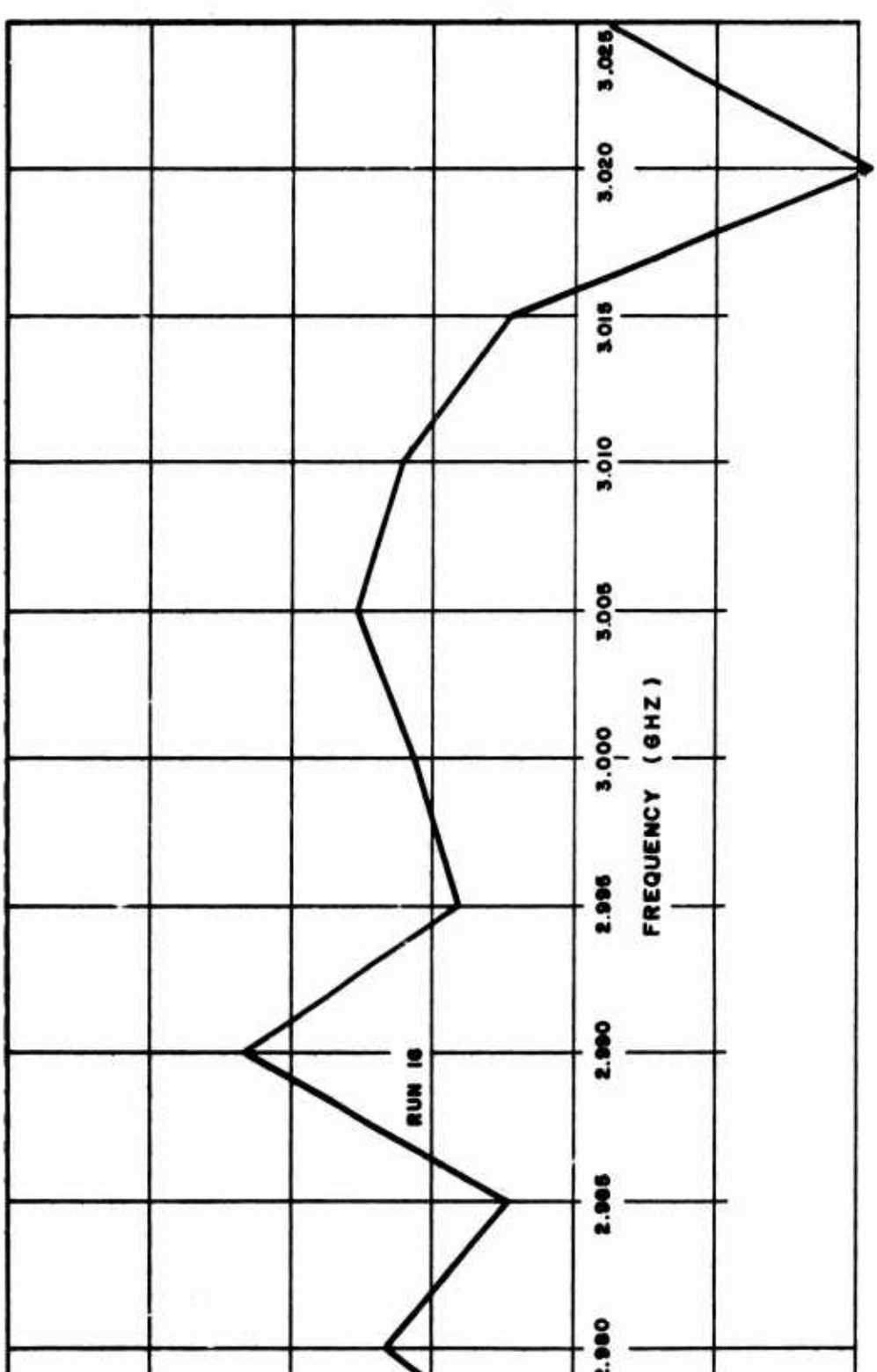

Figure 17. Phase vs. Frequency Characteristics of Klystron. Two Source Method. 4 September 1966, Run 16. VKG.

joined together through a well matched coaxial cable, having phase lengths approximately equal to that of the device under test, the line stretcher is adjusted to give an approximately horizontal phase vs. swept-frequency response on the oscilloscope or recorder. With the uniform length of coaxial cables removed and the test device inserted between the test terminals, a plot of phase vs. swept frequency is obtained, and the phase vs. frequency response of the system is used to correct the response obtained for the test device. Measurements of phase difference vs. frequency are made with respect to that obtained for the phase measurement system. This correction, in effect, calibrates out non-linearities due to reflection interactions and residual curvature of the phase measurement system. In this manner, accuracy is enhanced.

Run 17 shows a typical phase vs. swept frequency presentation of the phase measurement system itself. There is some phase curvature starting at about 3 GHz and ending about 3.007 GHz. This curvature is due to tunnel diode detector power sensitivity over this frequency range. Except for this "hump," the system itself is essentially linear. (Note: Tunnel diode detectors have now been replaced by a preamp/diode detector arrangement and the phase measurement system has essentially linear phase vs. frequency response from 2.975 to 3.025 GHz.) Phase non-linearity due to the detectors, system phase curvature, and reflection interactions are calibrated out of the final phase vs. frequency data by means of the calibration run.

2. Receiver Chain

Preliminary swept frequency phase testing began in May 1964 on the receiver chain shown in Figure 19. Under normal system operation, the echo return from the target is received at the slave site antenna, is amplified in a low noise S-band receiver chain, up-converted to X-band, further amplified and transmitted over a microwave link to the master site. At the master site, the up-converted signal and local oscillator signal are mixed and the resulting S-band signal is then processed to obtain angle information. The receiver chain test of Figure 19 contains the r-f portion of one slave site and the X- to S-band conversion equipment of the master site. Microwave path loss was simulated by the variable attenuator between the multiplexers. Since the shortest microwave link is over six miles in length, phase linearity cannot be tested across a microwave link. It would require a reference coaxial cable over four miles in length to equalize the time delay across the microwave link, and cost and attenuation would be prohibitive. All components were operated at their normal input power levels to simulate actual system operation. Attenuation was used judiciously throughout the chain to insure that all TWTs operated at least 15 db below input saturation levels.

Runs 18 and 19 of Figure 20 are repeated phase vs. CW swept-frequency measurements on the receiver chain. Run 19 was performed nine minutes after Run 18. The runs have been corrected for residual phase deviations. There is good correlation between the runs. Random noise-like phase deviations were present and this caused the two runs to be slightly different. These particular runs were made using a 10 second sweep, i.e., the total time to make the measurement was 10 seconds. Data was sampled at a faster rate (1-2 sec) but faster sweeps did not show much of the noise-like phase deviations. When phase was sampled at a 100 second rate, random phase perturbations were very distinct. Typical random phase fluctuations of ±1.5 degrees were observed. Over a period of two minutes, several large random phase jumps of ±5 degrees were observed. Phase fluctuations were partly due to ac

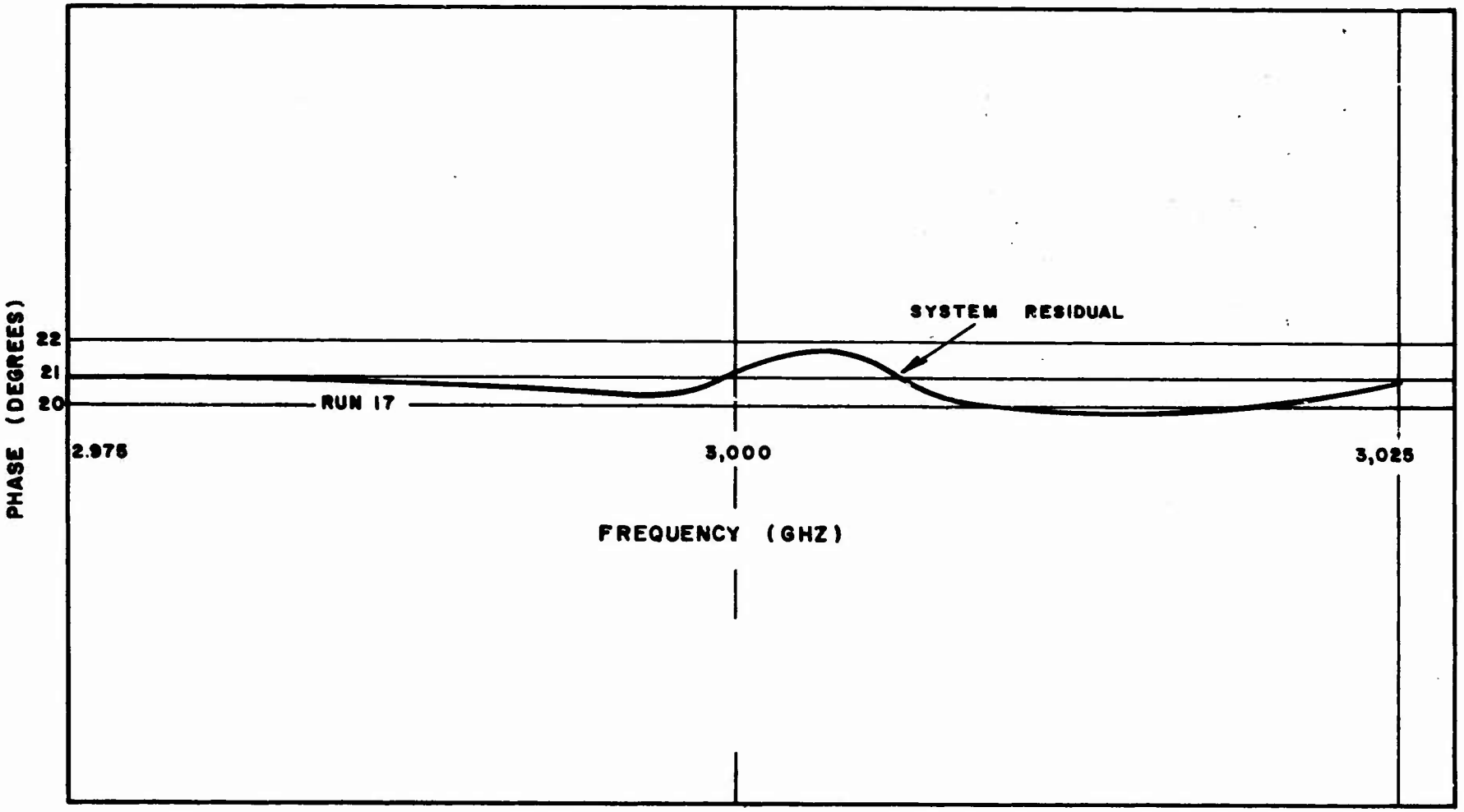

Figure 18. Phase vs. Swept Frequency of Phase Measurement System. Data Taken From X-Y Recorder Presentation. 31 July 1964, Run 17. VKG

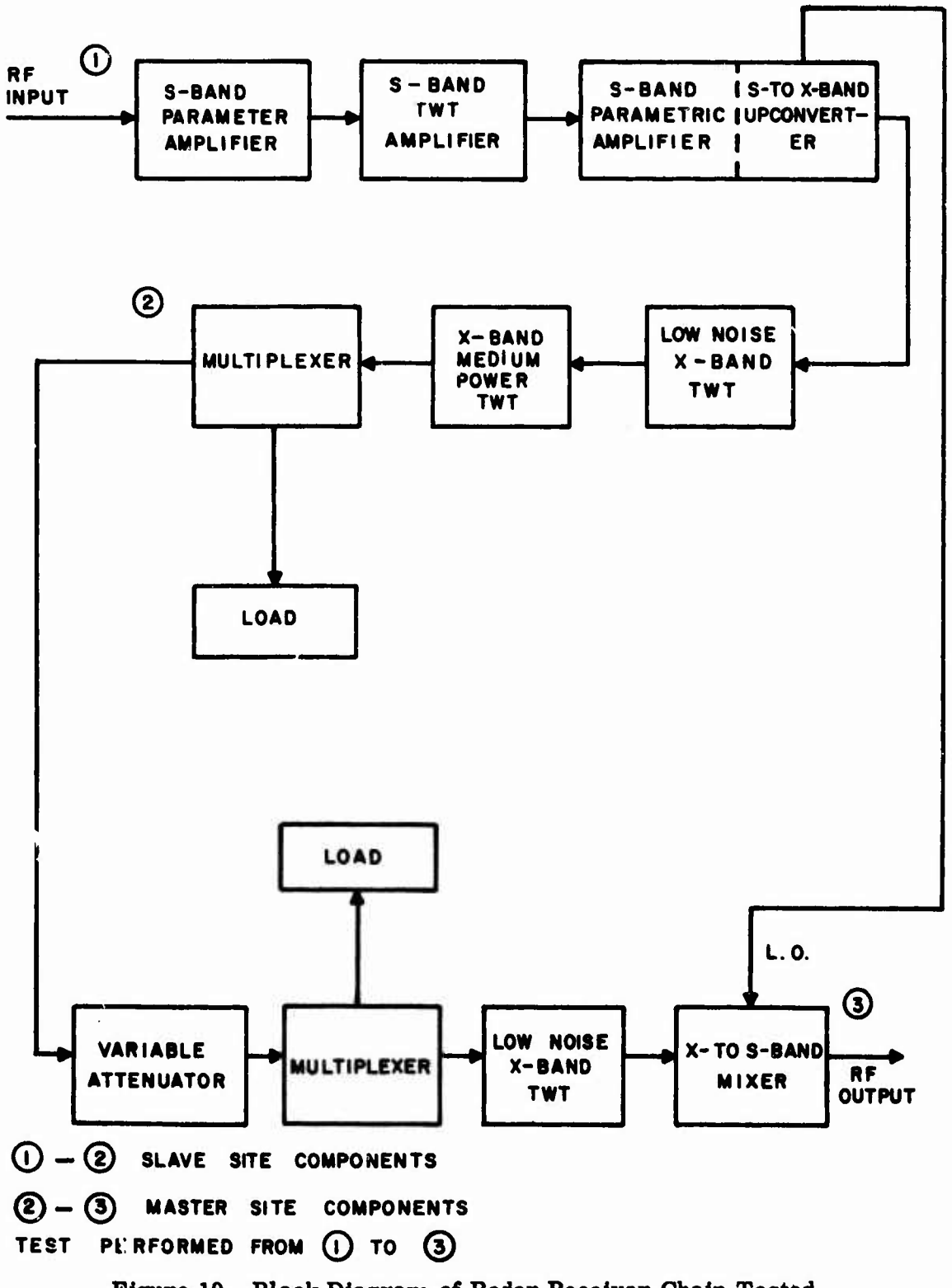

Figure 19. Block Diagram of Radar Receiver Chain Tested

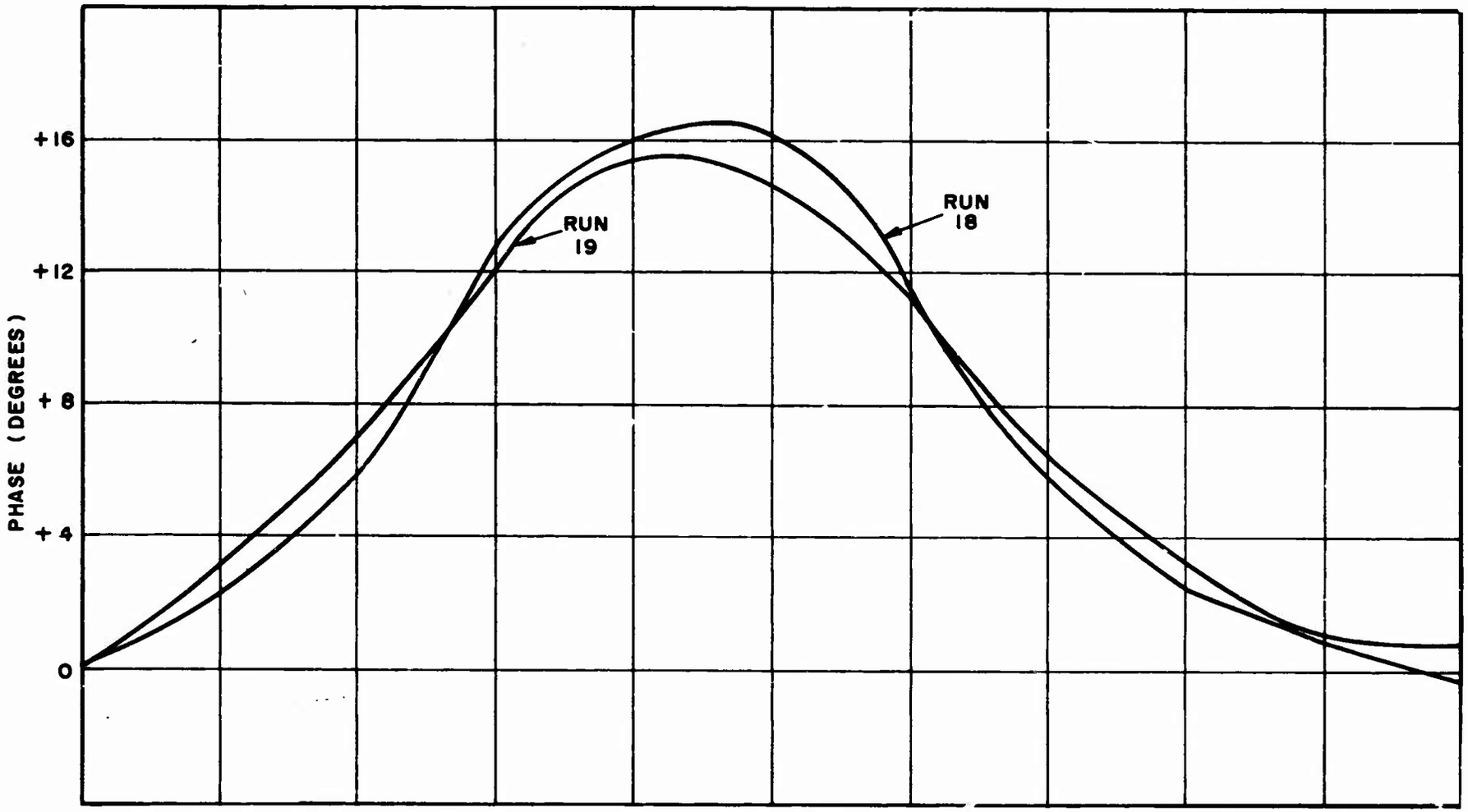

Figure 20. Phase vs. Frequency (Swept) of Receiver Chain. Runs 18 and 19, 19 May 1964. 10 Second Sweep. VKG.

line voltage transients. The X- and S-band mixer had excessive loss and the S-band output signal level was not far above the noise level. Part of the noise-like phase deviation is attributed to the noisy low level signal output from the X- to S-band mixer. The output port of the X- to S-band mixer had a high VSWR and this contributed to reflection interaction phase deviations. Several other equipment problems were discovered and corrected. Future data collected on this receiver chain showed that the chain did not have excessive phase non-linearity and the data was not noisy. The whole purpose of presenting the above discussion was to emphasize the following points:

(a) Phase vs. frequency tests can often be used as a diagnostic tool, i.e., if the phase vs. frequency characteristics show excessive perturbations, chances are that some component or components in the test system are not operating correctly or have excessive mismatch.

(b) Regulated beam voltages of traveling-wave tube amplifiers are often derived from the collector supply by means of several stages of Zener diode shut regulation. If the Zener diodes are voltage stabilized against ambient temperature changes by mounting the Zener diodes in a crystal oven, phase transients often occur when the oven turns on and off.

(c) The need for line voltage regulation of all test devices and phase measurement equipment cannot be overemphasized. Certain auxiliary equipment may not need its line voltage regulated but a rule-of-thumb is, when in doubt, regulate.

Phase tests on the receiver chain shown in Figure 19 were again performed in March 1965. The set up was modified slightly and the configuration is shown in Figure 21. Approximately 116 feet of RG 9 B/U coaxial cable was required to equalize the phase slope of the items tested. Run 20 of Figure 22 shows the phase vs. frequency characteristics of 116-foot lengths of coaxial cable in both the reference and test branches. Measurement was made on a low indicated phase reading scale. Phase deviations due to detector power sensitivity were negligible on this scale. Maximum phase deviations shown in Figure 22 are less than $.30^{o}$ which shows that coaxial cable is very nearly linear. The slight deviations are due to cable connectors. A 116-foot coaxial cable plus two type N adapters were used in the reference branch and three pieces of coaxial cable and three type N adapters were used in the test branch. The slight curvature is mainly due to the type N adapters interconnecting the various cables. Frequency was swept over a 60 MHz frequency band from 2.970 to 3.030 GHz.

Run 21 of Figure 23 shows the phase vs. swept frequency response of the overall receiver chain. Note that the maximum phase deviation across a 60 MHz frequency band centered at 3 GHz is less than 5 degrees. Five degrees maximum non-linearity is extremely good for a complex receiver chain containing as many devices as the one tested. It should be pointed out that the results shown in Figure 23 did not come automatically. Initial tests on the receiver chain started almost a week before the final test results shown were obtained. The parametric amplifiers were tuned for best phase response, primarily by tuning the varactor diode bias voltages. Many other system tests were performed to optimize bandwidth, gain, and phase linearity of the receiver chain. Again it was found that phase linearity test served as

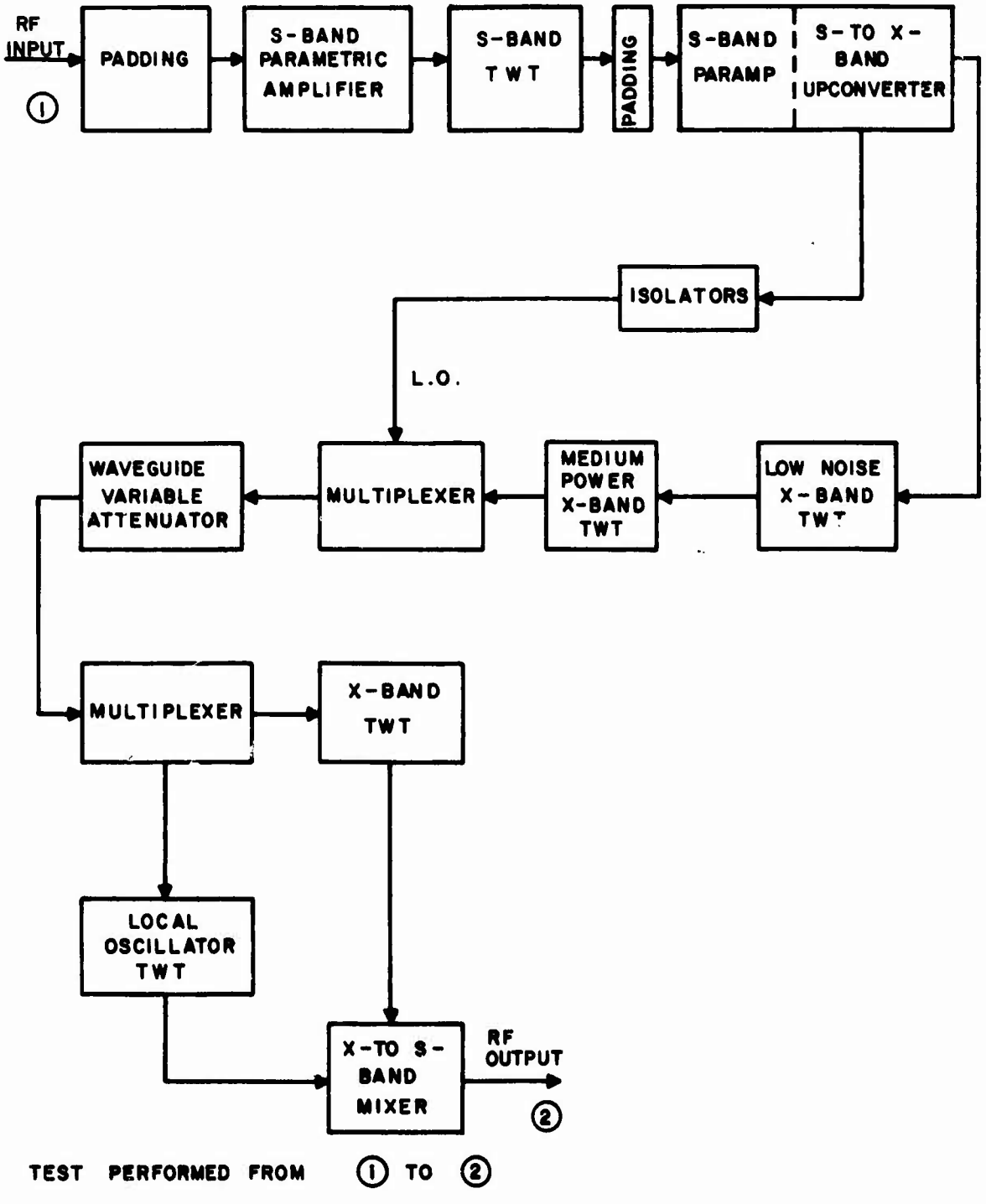

Figure 21. Block Diagram of Radar Receiver Chain Tested

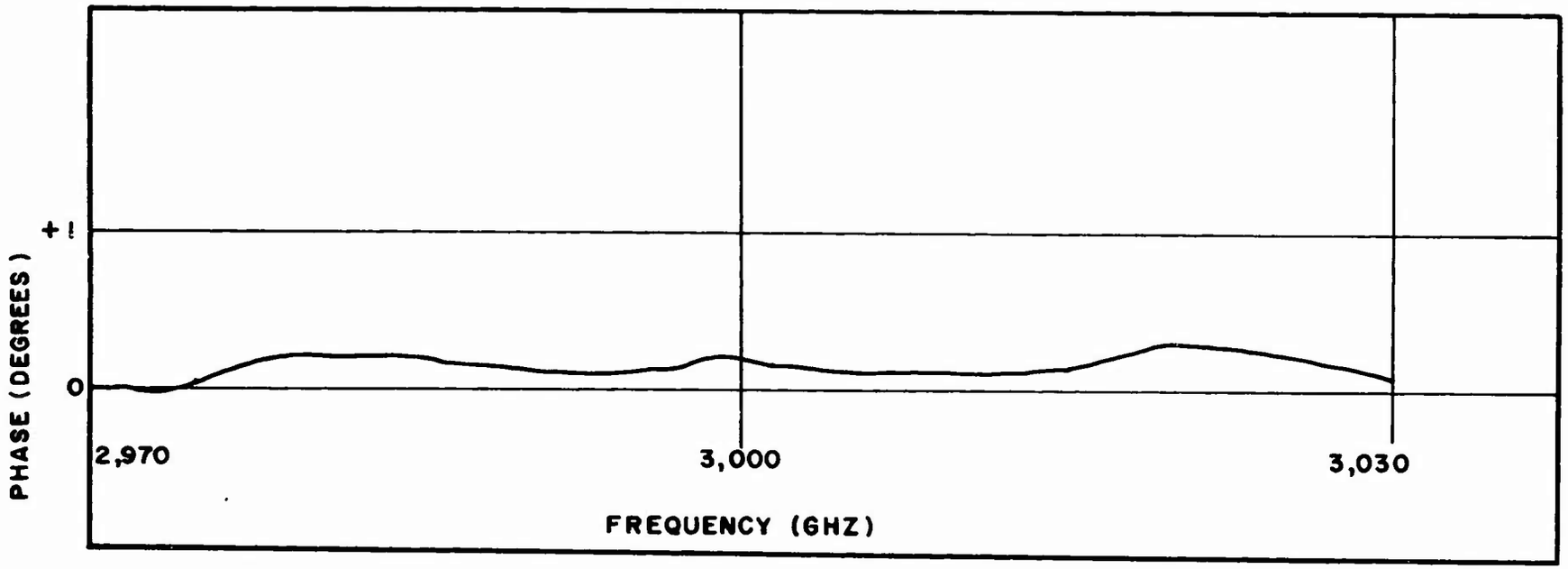

Figure 22. Phase vs. Frequency of 116-foot Lengths of RG-9 B/U Coaxial Cable. Plot Above Taken From Oscillogram 30 March 1965, Run 20. VKG.

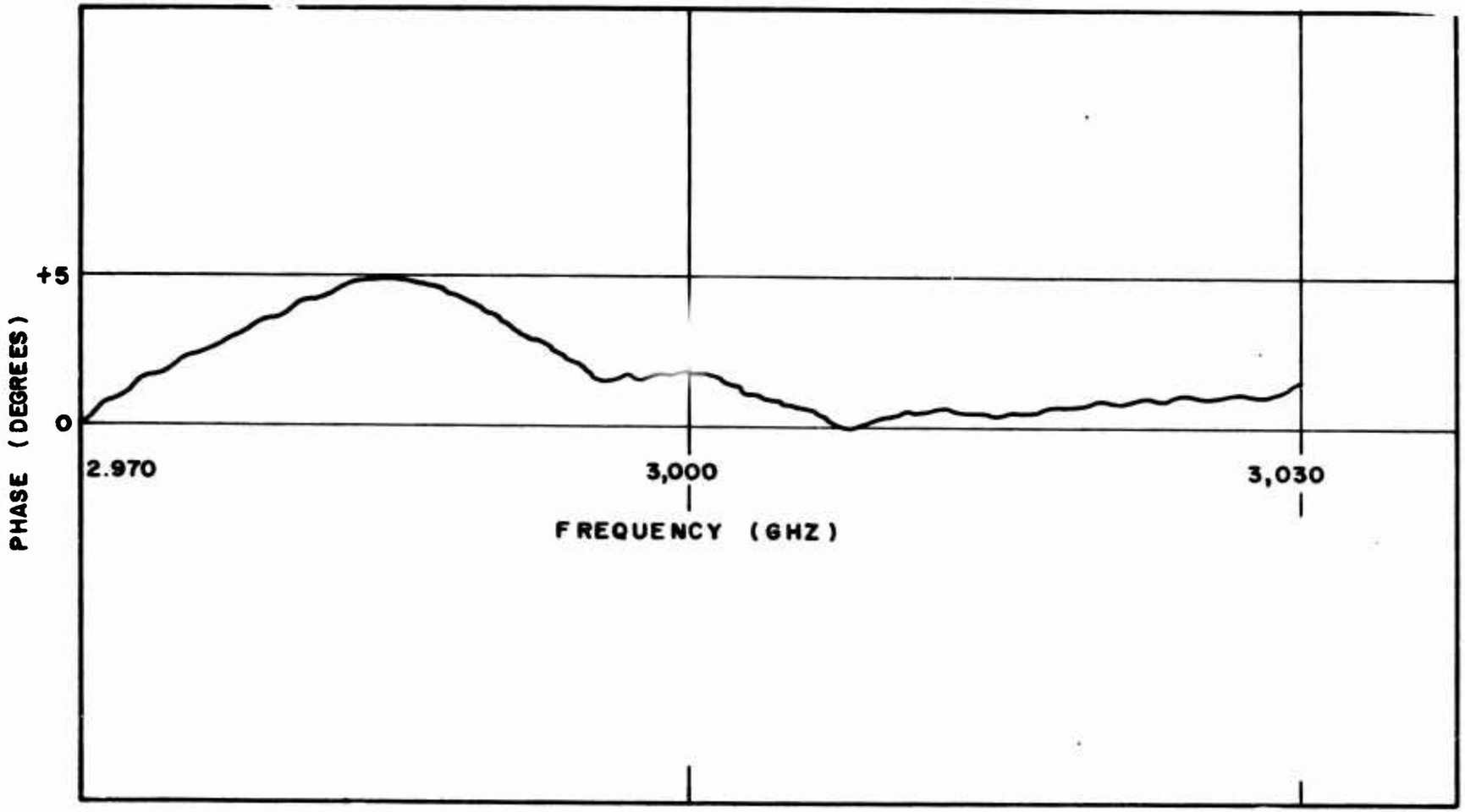

Figure 23. Phase vs. Frequency Characteristics of Radar Receiver Chain. Run 21, 30 March 1965. Plot Taken from Oscillogram Photograph. VKG.

a good diagnostic tool for finding problems in the receiver chain. Precautions listed previously were taken to obtain good results. Random noise deviations were approximately ±.3 degrees. Initially, the first S-band parametric amplifier had approximately 10 degrees peak-to-peak phase deviation across the frequency band (50 MHz). By tuning the bias voltage of the varactor diodes in the paramp (which essentially determines the band pass of the amplifier), phase deviation was improved to 1 degree peak-to-peak across the 50 MHz frequency band.

It should be mentioned that the amount of coaxial delay line required to equalize the phase slope of the device under test is easily determined using the following technique. The device to be tested is inserted in the test branch and frequency is swept over a known band. The time delay of the device under test can be calculated from the phase vs. frequency characteristic.

$$\tau_d = \frac{d_\phi}{d_\omega} \tag{14}$$

where

τ_d = time delay

ϕ = phase (degrees)

ω = frequency (radians/sec)

or for the case in point:

$$\tau_d \simeq \frac{\Delta\phi}{\Delta\omega} = \frac{\Delta\phi}{2\pi\,\Delta f} = \frac{\Delta\phi}{(360^o)\,\Delta f} \tag{15}$$

$\Delta\phi$ is the total change in phase from start to stop of the frequency sweep and Δf is the frequency difference between the start and stop frequencies. Equation 15 will give the approximate time delay of the device under test assuming that the phase non-linearity of the device under test is small.

The velocity of propagation in a coaxial cable whose conductors are completely immersed in a dielectric is, theoretically:

$$v = \frac{c}{\sqrt{\epsilon}} \tag{16}$$

where

c = velocity of light in a vacuum

ϵ = relative dielectric constant

RG 9 B/U coaxial cable has a polyethylene dielectric with $\epsilon \simeq 2.3$. Using this value in equation 16 gives a value for v/c of .66. Using a value of 9.84×10^8 ft/sec for c, the time delay of one foot of coaxial cable can be calculated from the following equation:

$$\tau_1 = \frac{L}{v} \tag{17}$$

where L is the length in feet (one foot) and v is the velocity of propagation (9.84×10^8 ft/sec $\times$ .66) the time delay of one foot of RG 9 B/U coaxial cable is, from equation 17:

$$\tau_1 = \frac{1 \text{ foot}}{(9.84 \times 10^8 \text{ ft/sec})\,(.66)} \simeq 1.54 \text{ nanoseconds} \tag{18}$$

Using the time delay of the device calculated from equation 15, the reference delay cable length in feet is obtained by dividing τ_d by 1.54 nanoseconds/foot.

The above technique was used in measuring the time delay of test devices and cable lengths. The results obtained compared favorably with that obtained by other techniques of measuring time delay and with theoretical calculations. Theoretical calculations of time delay and measured values agreed to within .1 nanoseconds.

3. Cascaded Parametric and Traveling-Wave Tube Amplifiers

Phase linearity measurements were conducted on the master site S-band r-f receiving chain on 31 July 1964. This chain consists of a S-band parametric amplifier and two traveling-wave tube amplifiers. 60 db attenuation was placed at the parametric amplifier input to maintain the TWT input power levels at least 15 db below saturation, and 10 db attenuation was placed at the output of the second TWT to minimize reflection interaction effects and provide the proper power level into the phase measuring system. The test was performed using CW swept-frequency operation. The results of the test are shown in Figure 24. Runs 22 and 23 are two repeated runs on the test device. The two runs were repeatable to within .1°. The slight phase differences in the two runs are due to a small time delay change in the chain that resulted in a level shift of one of the runs. Correction of Runs 22 and 23 for residual phase curvature was not necessary since the runs showed that the devices were linear enough to meet system requirements. A block diagram of the test devices is given in Figure 25.

4. Traveling-Wave Tube Amplifier

Phase linearity tests were performed on the traveling-wave tube amplifier which is part of the ASFIR transmitter on 20 August 1964. The items included in this test are shown in Figure 26.

The results of the test are shown in Figure 27. Runs 24 and 25 are repeated runs on the items shown in Figure 26. The two runs would be superimposed except for a time delay change in the TWT that shifted the two curves. The results show that this particular portion of the transmitter will easily meet system phase linearity requirements.

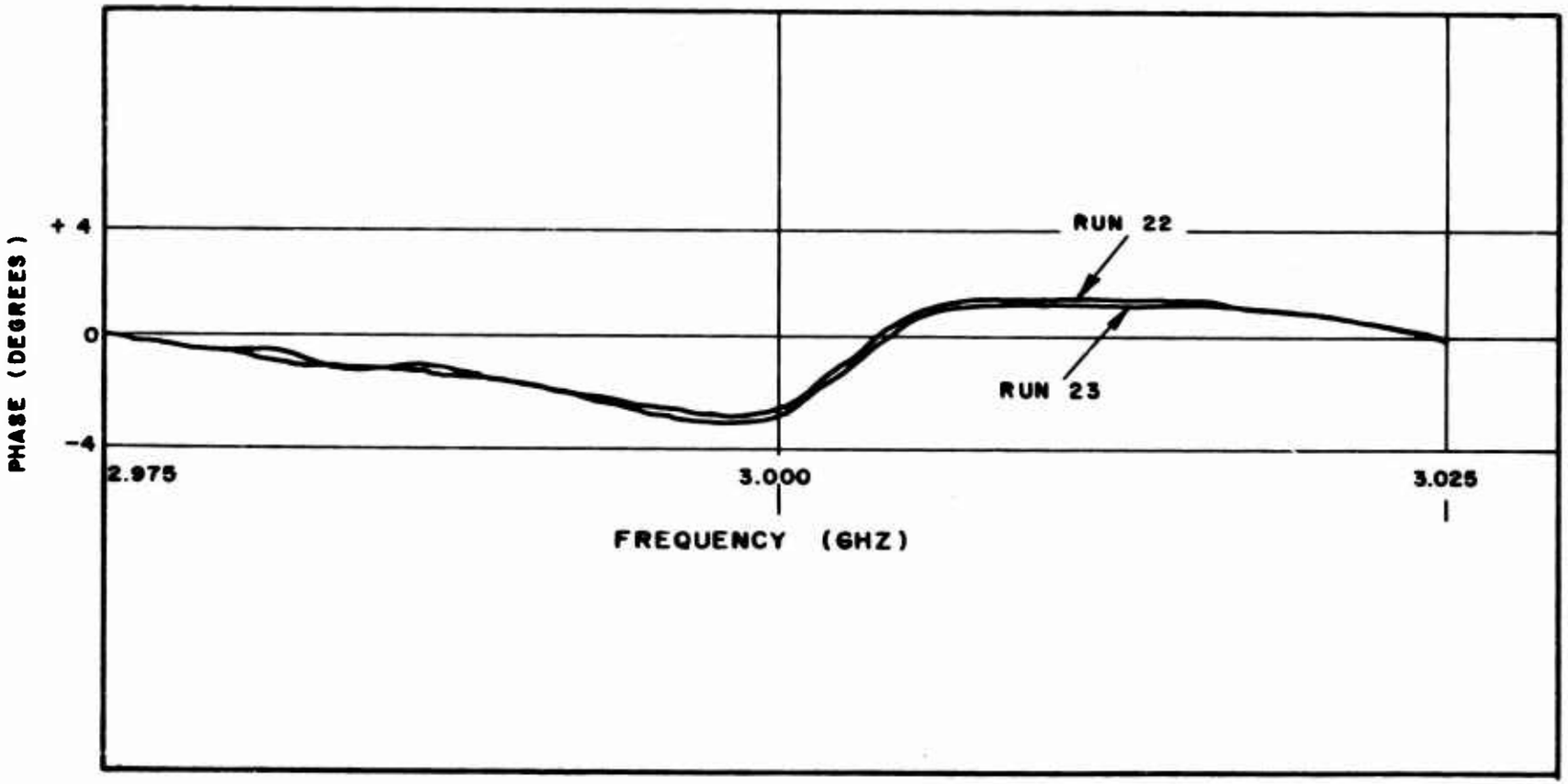

Figure 24. Phase vs. Frequency Characteristics of S-Band Receiver Chain. Runs 22 and 23, 31 July 1964. Plot taken from Recorder Presentation. VKG.

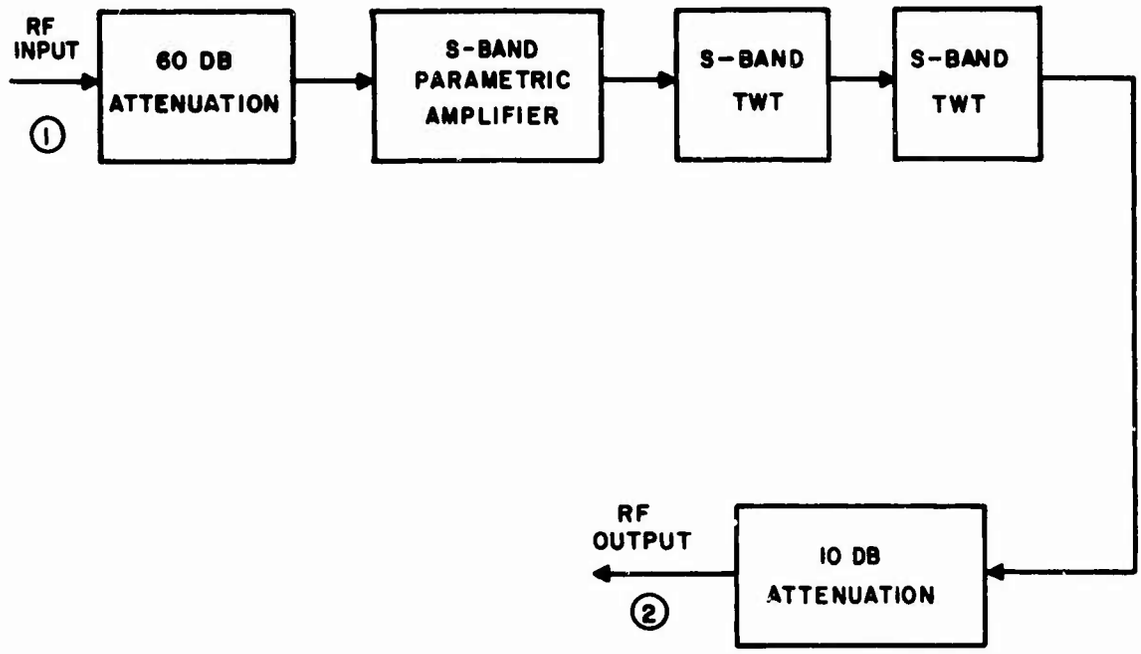

Figure 25. Block Diagram of Master Site RF Receiver Chain Test

5. Microwave Link

A rather intersting round-trip experiment was conducted on 3 December 1964. The test arrangement is shown in Figure 28. A phase-locked 3 GHz CW signal was transmitted from the master site across a microwave link of approximately 6 1/4 miles. The received signal was amplified at the slave site and transmitted back to the master site. The signal received at the master site was down-converted to 3 GHz and compared to a reference signal in the phase measurement system. A plot of phase variations vs. time was obtained using a recorder presentation. Figure 29 shows the results of this test. Noise, like phase deviations, were typically 3 degrees peak-to-peak. The general phase pattern was somewhat sinusoidal in nature over the seven-minute recorded time period and showed about one cycle/minute phase variation. Equating phase variations to time delay variations across the microwave link (assuming that frequency is constant) gives a time delay variation of approximately ±.003 nanoseconds over the seven-minute recorded time period. This is a very interesting result since it shows that the error involved due to time delay changes across the link will be very small during normal system operation.

The short term frequency stability of the phase-locked source was ±30 cps. Assuming that the time delay across the link is constant, phase deviations due to short term frequency stability is a maximum of ±.86°. The absolute phase length across the link is many millions of degrees. It is remarkable that the observed phase variations across the link were only about ±3°.

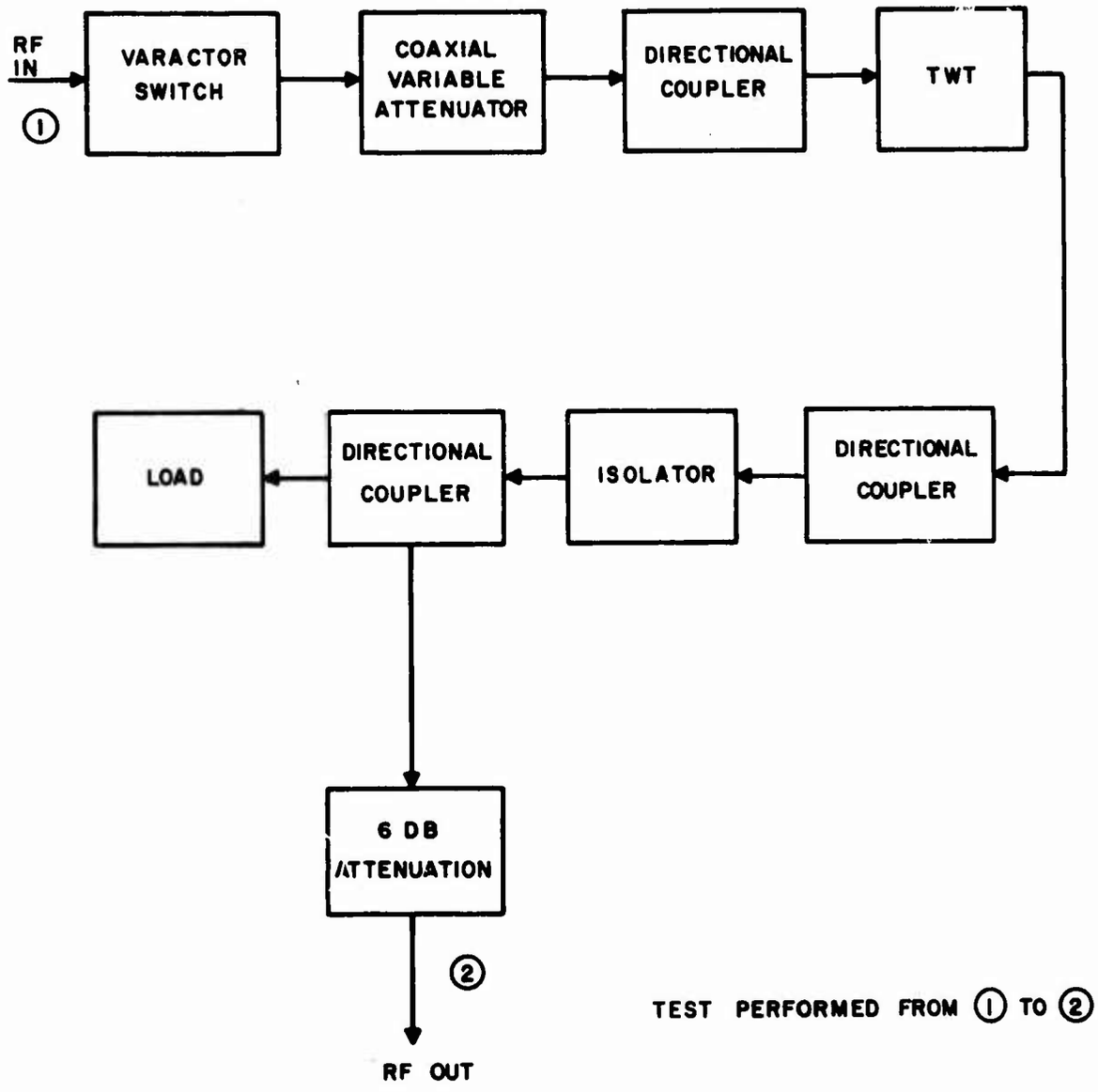

Figure 26. Block Diagram of Traveling-Wave Tube Amplifier Test Arrangement

Several degrees of noise-like phase deviations are to be expected. This is due to phase instabilities of the active devices, and noise contributions in the equipment and across the microwave link. Light snow was falling during the test, but it did not seem to have much effect on the phase deviations observed. When all equipment at the slave site except the devices used in the test were turned off, the same sinusoidal phase variations were observed, but the time delay changed. This change in time delay was calculated to be .005 nanoseconds/minute. This change is extremely small. The phase-locked oscillator went into a search mode several times during the test run. The change in phase due to frequency deviations in the search mode was typically 15 degrees.

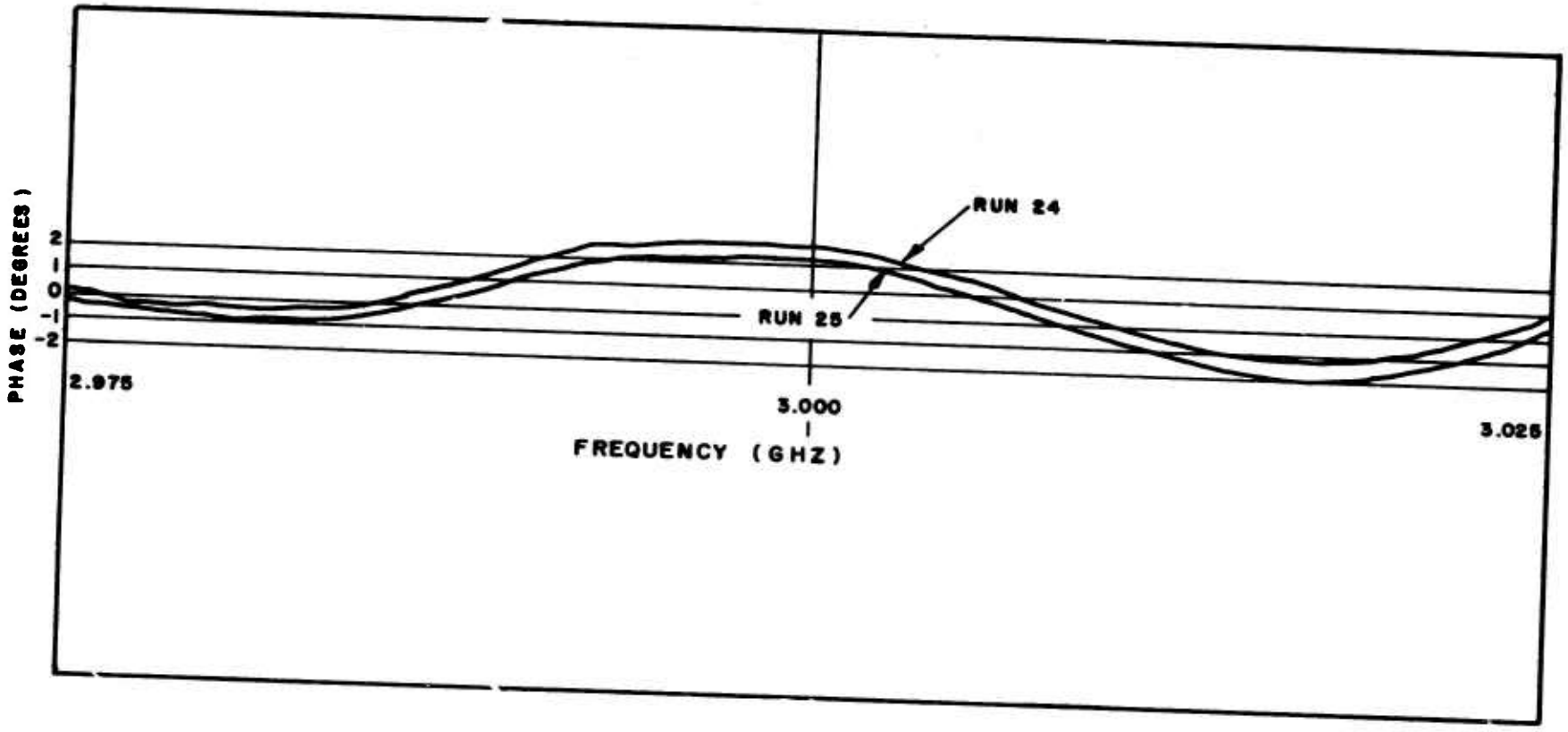

Figure 27. Phase vs. Frequency Characteristics of Traveling-Wave Tube Amplifier and Interconnecting Passive Devices Shown in Fig. 12. Runs 24 and 25, 20 August 1964. Plots Taken from Recorder Presentation. VKG.

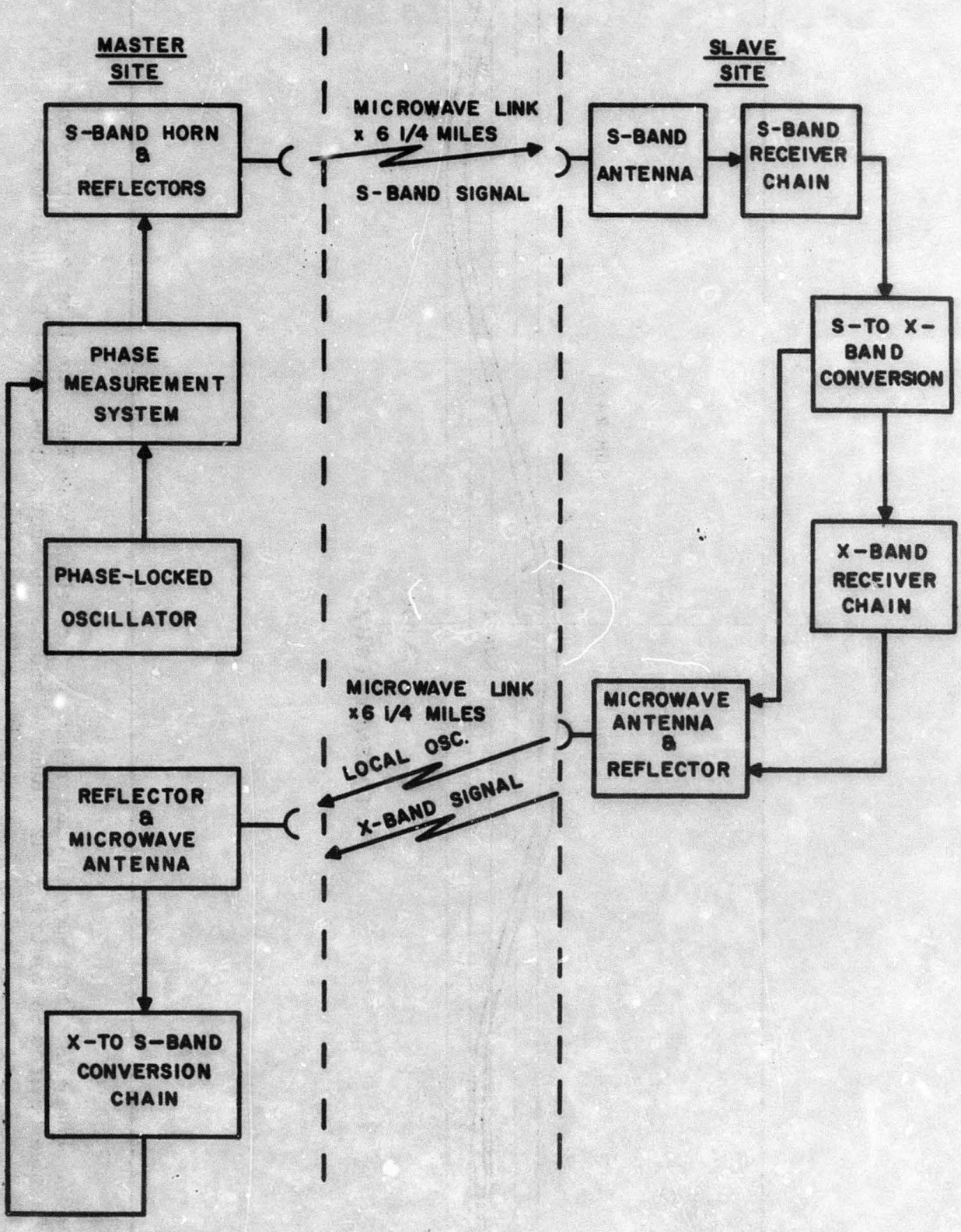

Figure 28. Block Diagram of Microwave Link Test

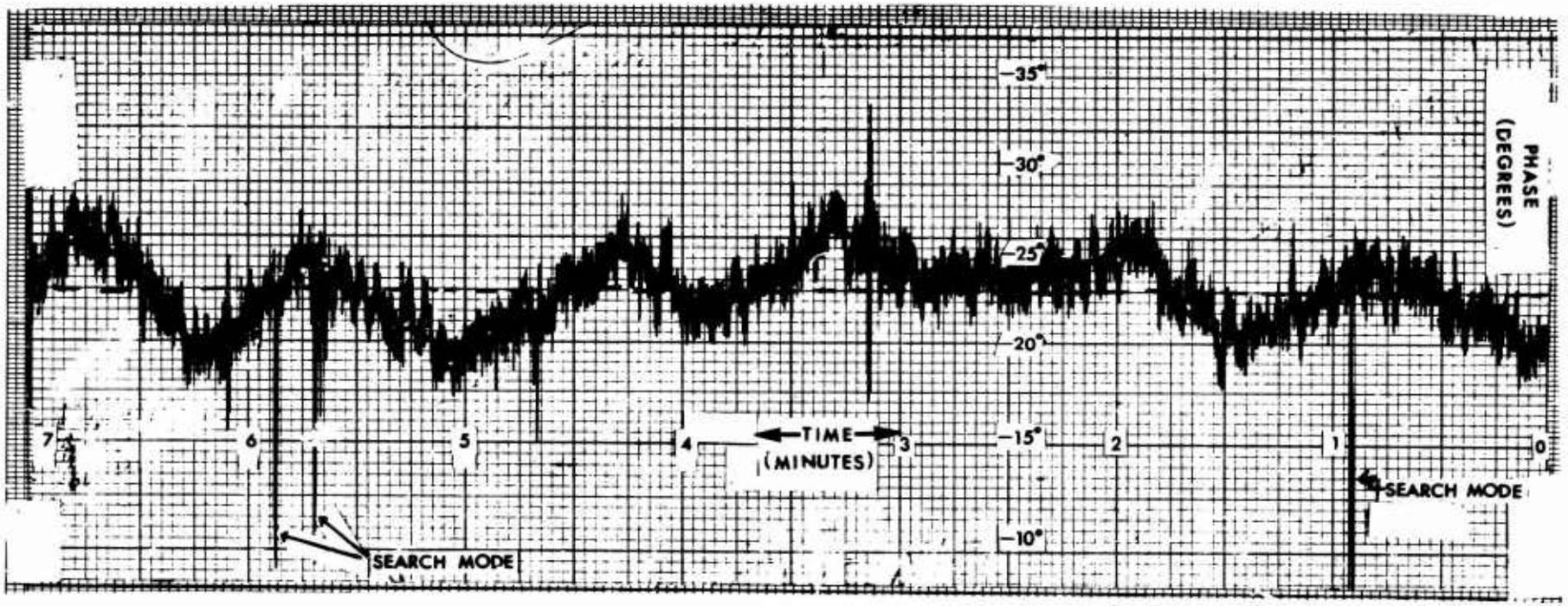

Figure 29. Phase Deviations vs. Time of Round-Trip Microwave Link Test. Run 26. 3 December 1964. VKG.

To minimize time delay variations (phase variations) all active devices in a receiver chain should be operated from a regulated source.

6. Klystron and Transmitter

Previous tests using the slotted-line detector showed that a large percentage of the phase non-linearities of the overall transmitter were due to phase non-linearities in the seven-cavity transmitter klystron. Phase measurements showed that klystron phase perturbations were greater by as much as a factor of seven over theoretical calculations that were conducted during klystron design. Since a klystron with linear phase vs. frequency response would result in a significant improvement to system performance, an attempt was made in March 1965 to mechanically time the seven cavities of the klystron.

Figure 30 is a block diagram of the circuit arrangement used for klystron tests. Phase measurements were made using pulsed signals in both reference and test branches. See Section III-C-2 of this report for a discussion of this operation. A pulsed linear FM signal of 2.4 milliseconds duration was used. Frequency was swept linearly from 2.975 to 3.025 GHz within the pulse; PRF rate was 100. The traveling-wave tube amplifier (TWT) serves two purposes in the transmitter. It can be used for phase connections and it provides input drive power to the klystron. For klystron tests, it was not part of the device tested. This is shown in Figure 30. It simply provided sufficient input drive to obtain maximum output power from the klystron.

Phase vs. frequency characteristics of the klystron as well as bandpass and power output were monitored simultaneously. The klystron tested on 9 March 1965 had a somewhat sinusoidal phase deviation of +7 and -4 degrees or 11 degrees peak-to-peak across the frequency band.

When the klystron was tuned for power output (amplitude flatness), the phase variation across the 50 MHz frequency band was again sinusoidal in nature and had approximately 8 degrees peak-to-peak deviation. Upon tuning for best phase linearity, peak-to peak phase deviation across the band was about 3 degrees.

In January 1966, another klystron was tuned for linear phase vs. frequency characteristics. The klystron that had previously been tuned in March 1965 was also tested. A test run was made on the components and phase measurement equipment without the klystron in the test arrangement. The results are shown in Run 27. Note that phase deviations due to the phase measurement system and components are a maximum of 1.5 degrees across the band. Test operation was pulsed linear FM. Frequency was swept linearly within a 2.3 millisecond pulse from 2.975 to 3.025 GHz. A different PRF rate (62) was used instead of 100 to minimize beating effects of the 1000 cps phase signals with harmonics of the PRF. The residual test arrangement was (1) - (3) - (4) in Figure 30.

Run 28 shows the phase vs. frequency characteristics of the klystron. Maximum phase deviation is 2.5 degrees. If the data is corrected for residual phase curvature, klystron phase deviations are less than 4 degrees across a 50 MHz frequency band. This test showed that the klystron had retained its phase response

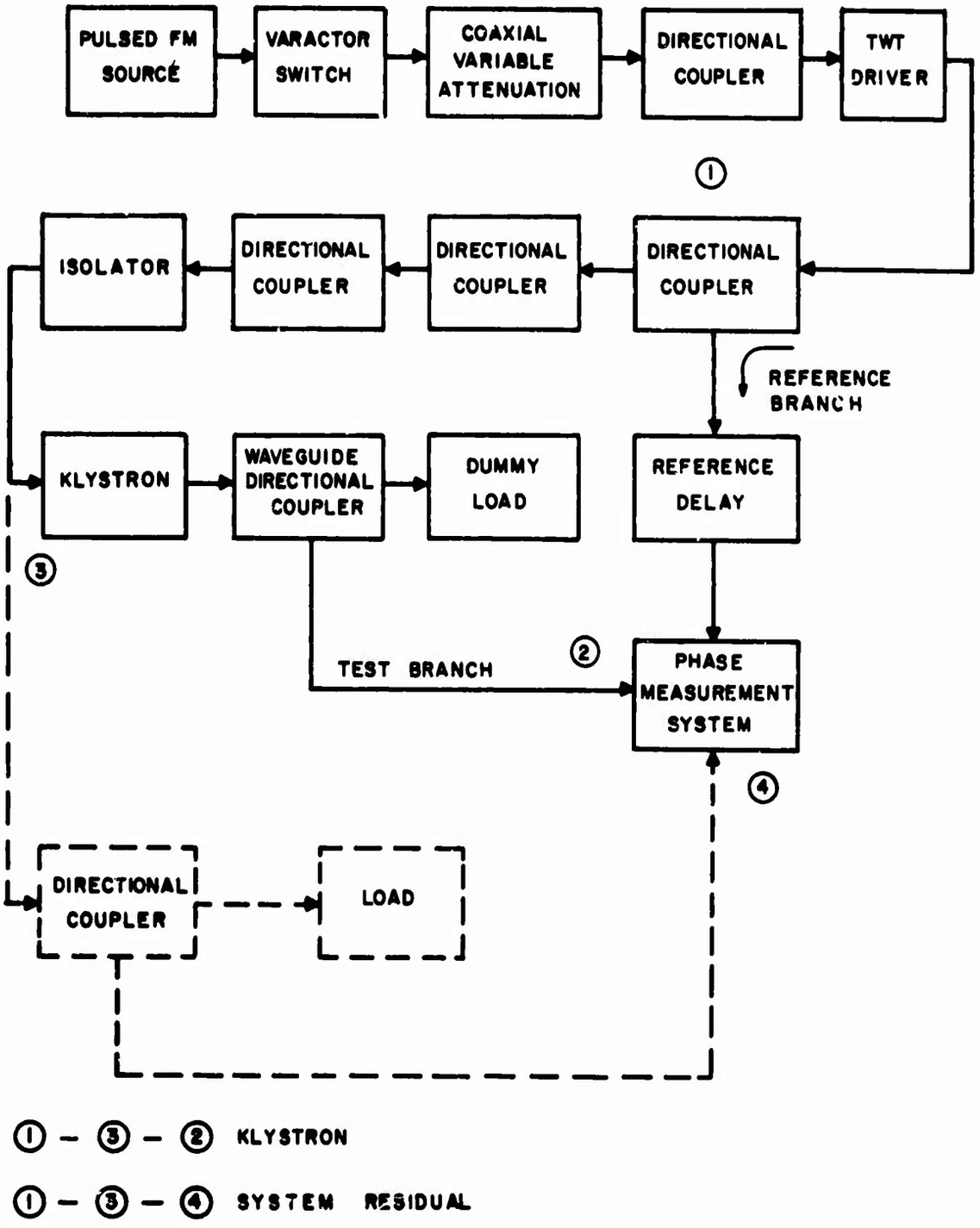

Figure 30. Block Diagram of Transmitter Klystron Tests

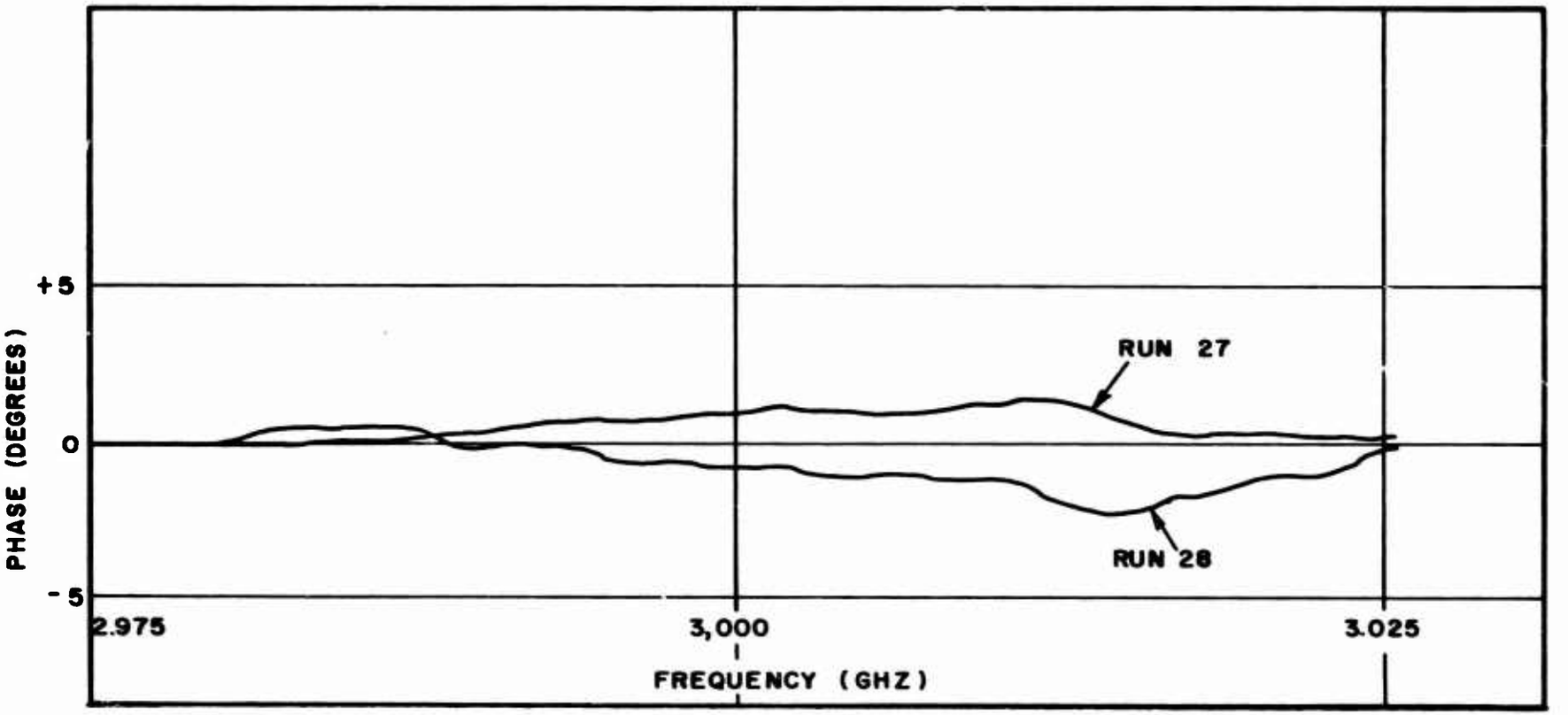

Figure 31. Phase vs. Frequency Characteristics of Transmitter Klystron. 14 January 1966. Run 27 is "Residual" and Run 28 is Klystron (tuned) Characteristics, 39 KV Beam Voltate, Klystron in Saturation. Plots Taken from X-Y Recorder Presentation. VKG.

characteristics during the ten months which had elapsed since it had been tuned. The circuit arrangement for klystron tests is (1) - (3) - (2) in Figure 30.

Runs 29 and 30 of Figure 32 show the phase vs. frequency characteristics of the transmitter klystron for different beam voltages. A maximum of .5 degrees difference between the two runs is attributed to external factors. It is seen from the curves that varying beam voltage 1000 volts changed the phase characteristics of the klystron very little (less than 1 degree maximum change). It did, however, change the time delay through the klystron. The time delay change was equalized by adjusting the line stretcher and superimposing the two curves.

Runs 31 and 32 of Figure 33 are curves of phase vs. frequency taken from an X-Y recorder presentation. Run 31 was made with the klystron in hard saturation. Run 32 was made with the klystron operating with an input drive level 2 db below that required to drive the klystron into saturation. The two curves have the same general shape. Maximum variation between the two curves is less than two degrees and the two curves are within $.5^{0}$ over 70 percent of the frequency band. Changing the drive level into the klystron did have some effect on the phase vs. frequency characteristics, but changes were small.

Test runs were also performed to observe the effect of varying magnet currents upon phase linearity. Varying magnet currents ±10 percent from nominal settings changed the phase response less than 1.5 degrees across the frequency band.

Phase vs. frequency characteristics of the transmitter klystron that was tuned for minimum phase deviations across the operating frequency band in January 1966 are shown in Figure 34. Run 33 shows the phase response of the transmitter klystron before tuning. Maximum deviation from linear response is 16.8 degrees. Run 34 of Figure 35 shows the phase response of the transmitter klystron after the seven cavities have been tuned to give maximum amplitude flatness across the 50 MHz operating frequency band. Maximum deviation is now +7 and -2.6 degrees or 9.6 degrees peak-to-peak. It should be noted that tuning the klystron for maximum amplitude flatness resulted in a phase linearity improvement of about 2:1, when compared to initial phase deviations of the klystron.

Runs 35 and 36 are repeated runs showing the phase vs. frequency characteristics of the klystron after tuning for minimum phase distortion. Phase linearity has been significantly improved. Maximum phase deviation from linear response is now +2.6 and -1.6 degrees or 4.2 degrees peak-to-peak. Run 36 was a repeated check of Run 35 in which the line stretcher was adjusted to observe reflection interaction effects and equipment measurement errors. The two curves were superimposed mathematically for report purposes. The two runs show essentially the same phase vs. frequency characteristics.

It was noted that tuning the klystron for minimum phase deviations resulted in a value of output power approximately 1 db lower than the maximum power output capability of the klystron.

Tests performed on the overall transmitter after the klystron had been "phase" tuned showed a maximum deviation of $\pm 3^{0}$ across the operating frequency band. Phase

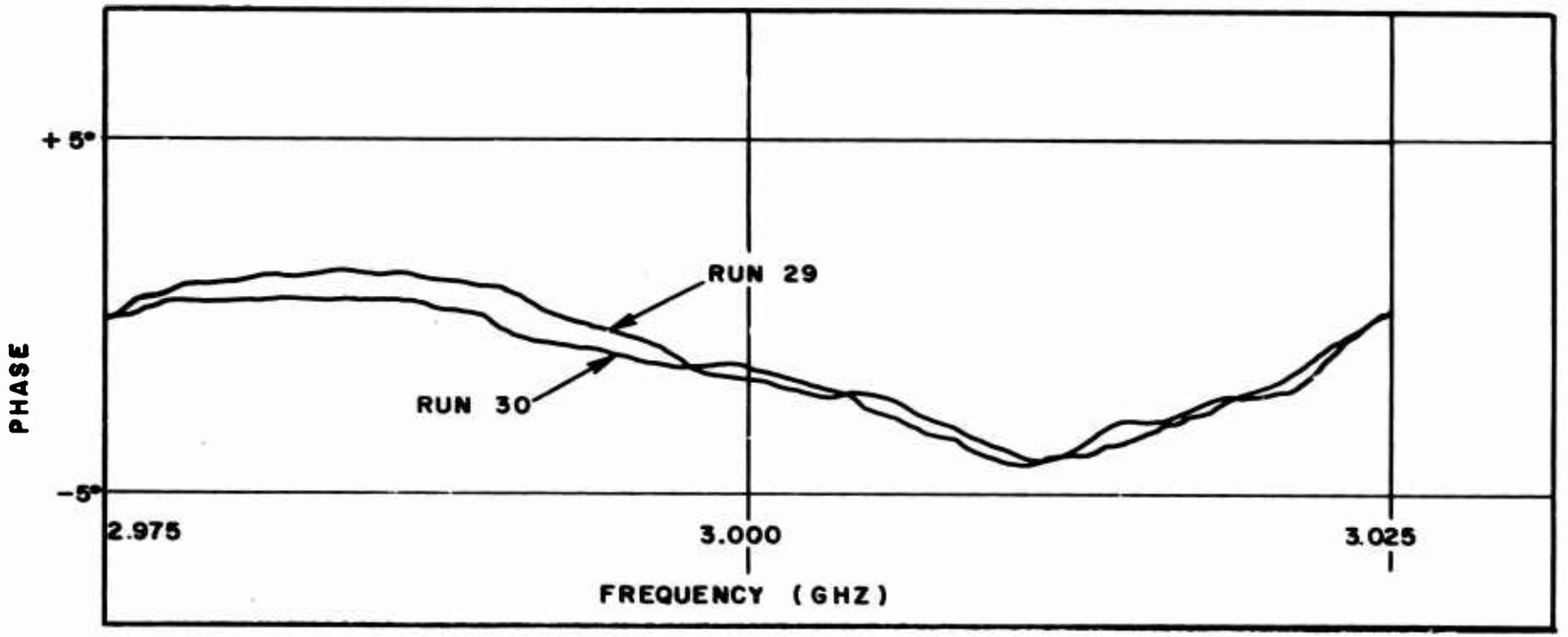

Figure 32. Phase vs. Frequency Characteristics of Transmitter Klystron. 14 January 1966. Run 29 was for Beam Voltage of 37 KV. Run 30 was for Beam Voltage of 38 KV. Plots Taken from X-Y Recorder Presentation. Shows Effects of Varying Beam Voltage. VKG.

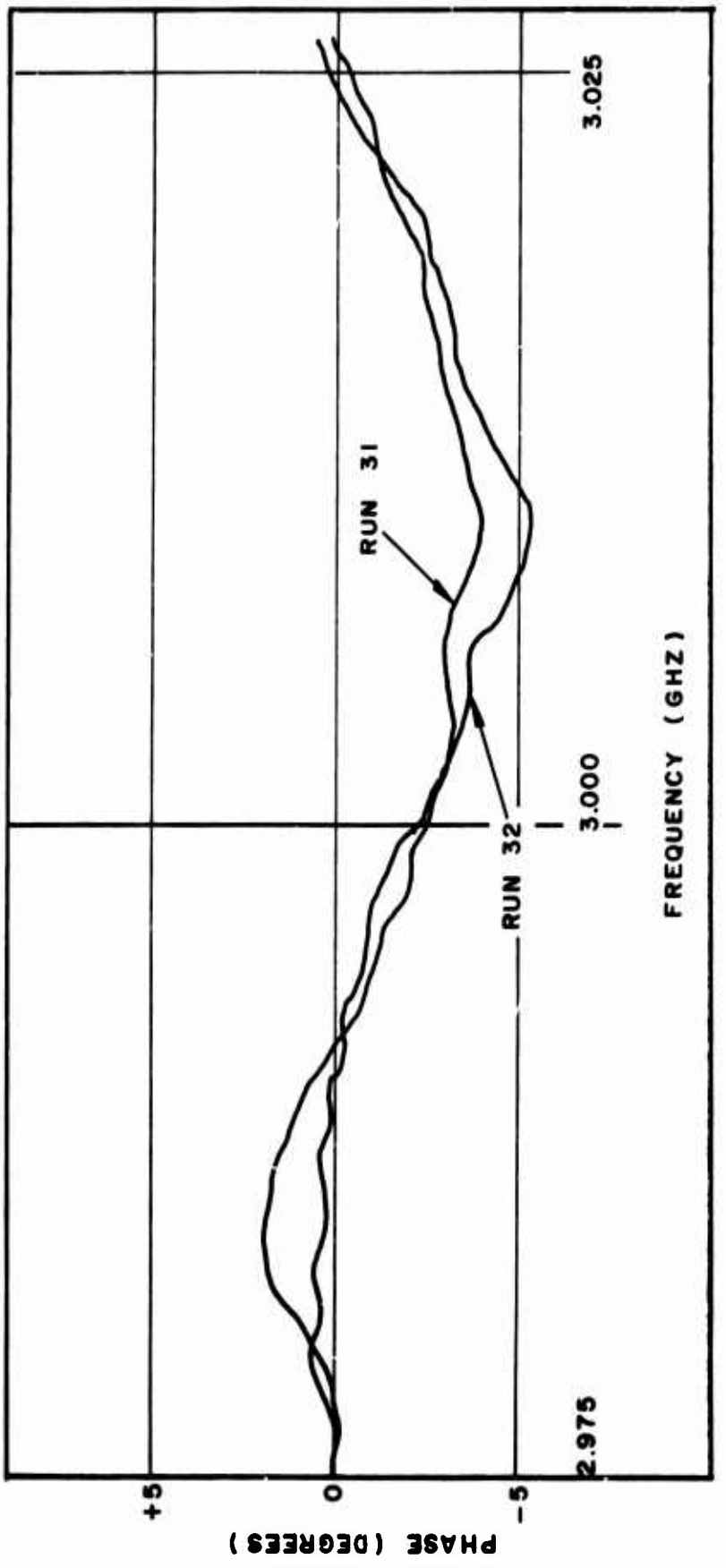

Figure 33. Phase vs. Frequency Characteristics of Transmitter Klystron. 14 January 1966. Beam Voltage for Both Runs was 39 KV. Run 31 was Klystron in Saturation. Run 32 had Klystron 2 DB from Saturation Effects of Varying Klystron Drive. VKG.

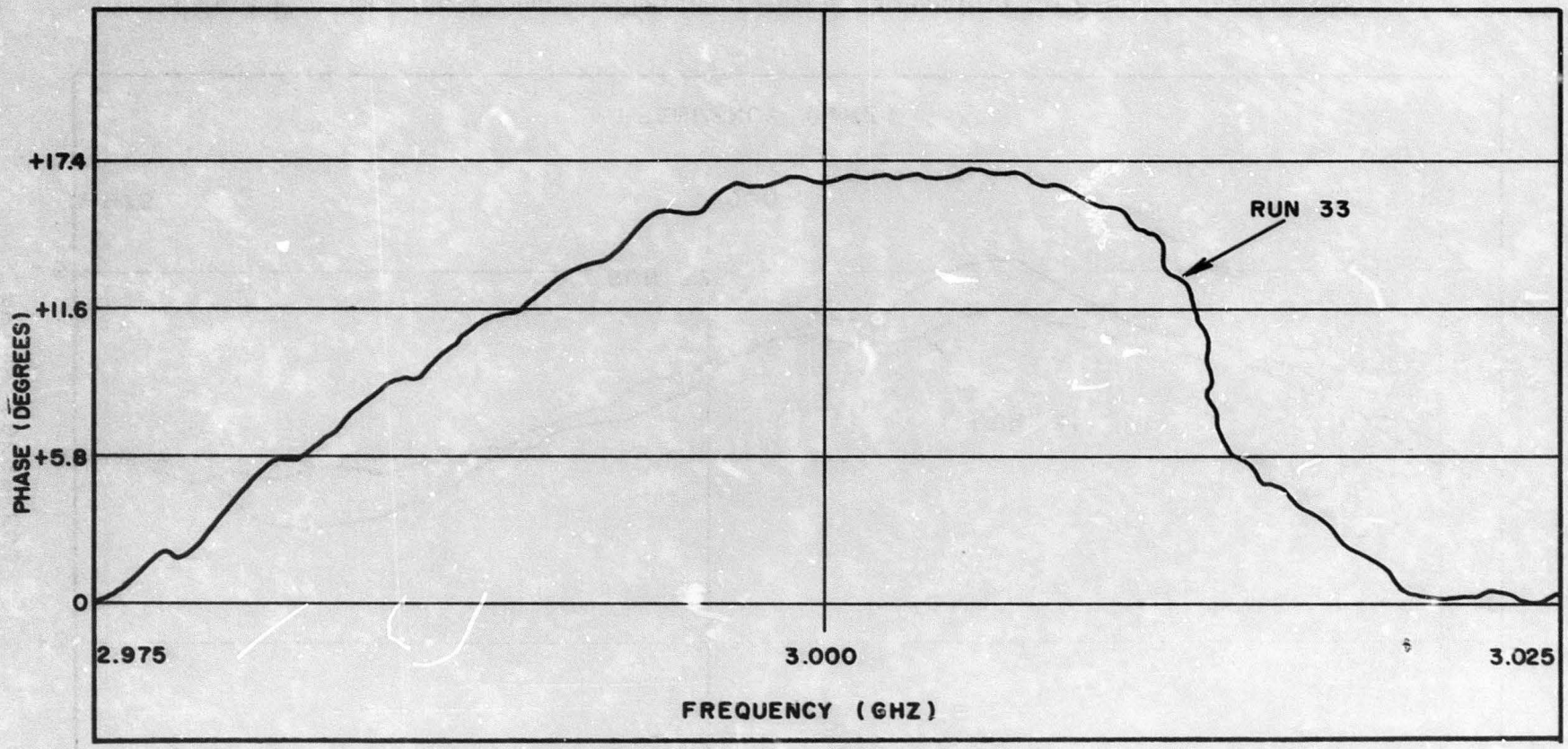

Figure 34. Phase vs. Frequency Characteristics of Transmitter Klystron. 11 January 1966. Klystron Phase Characteristics Before Phase Tuning. Run 33. VKG.

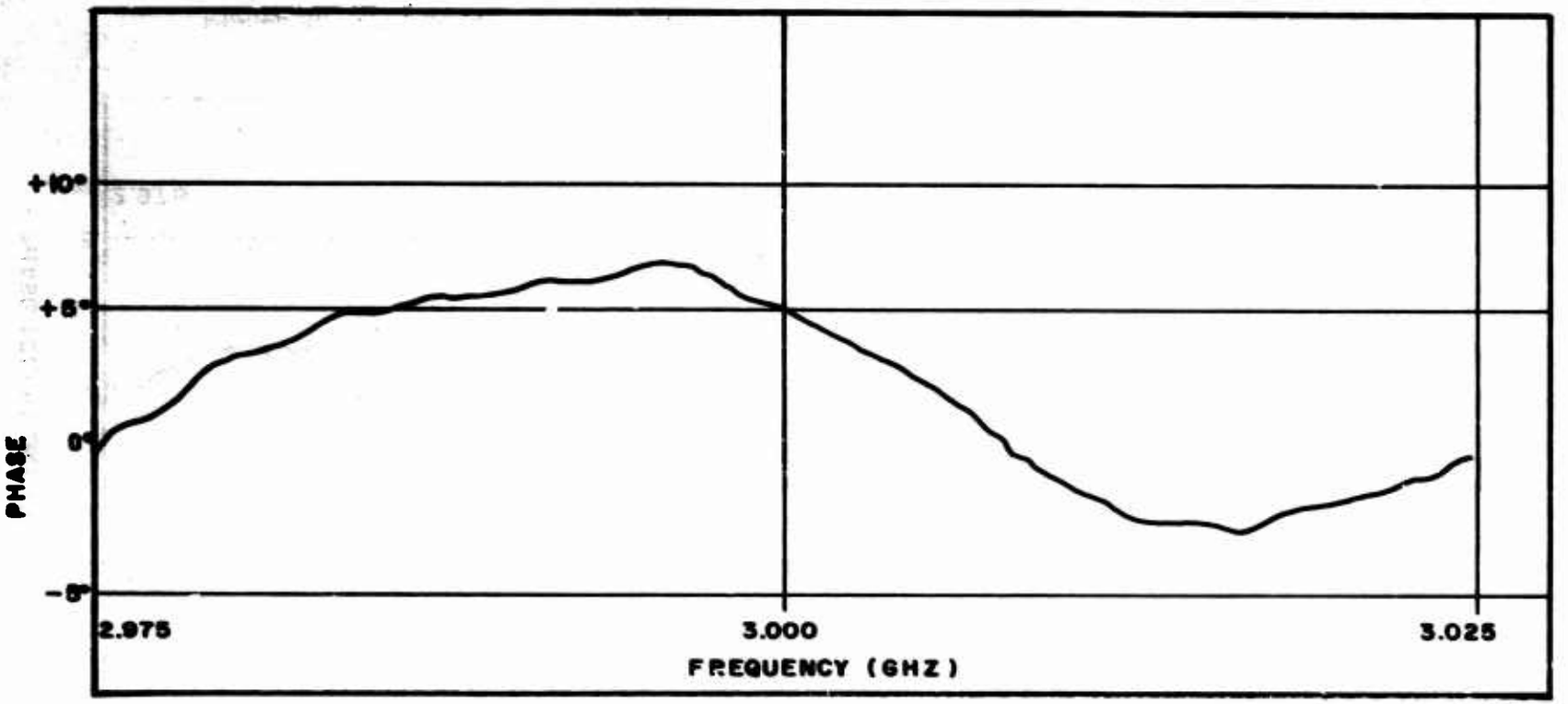

Figure 35. Phase vs. Frequency Characteristics of Transmitter Klystron. 12 January 1966. Klystron Cavities Adjusted for Maximum Amplitude Flatness Across Band. Run 34. VKG.

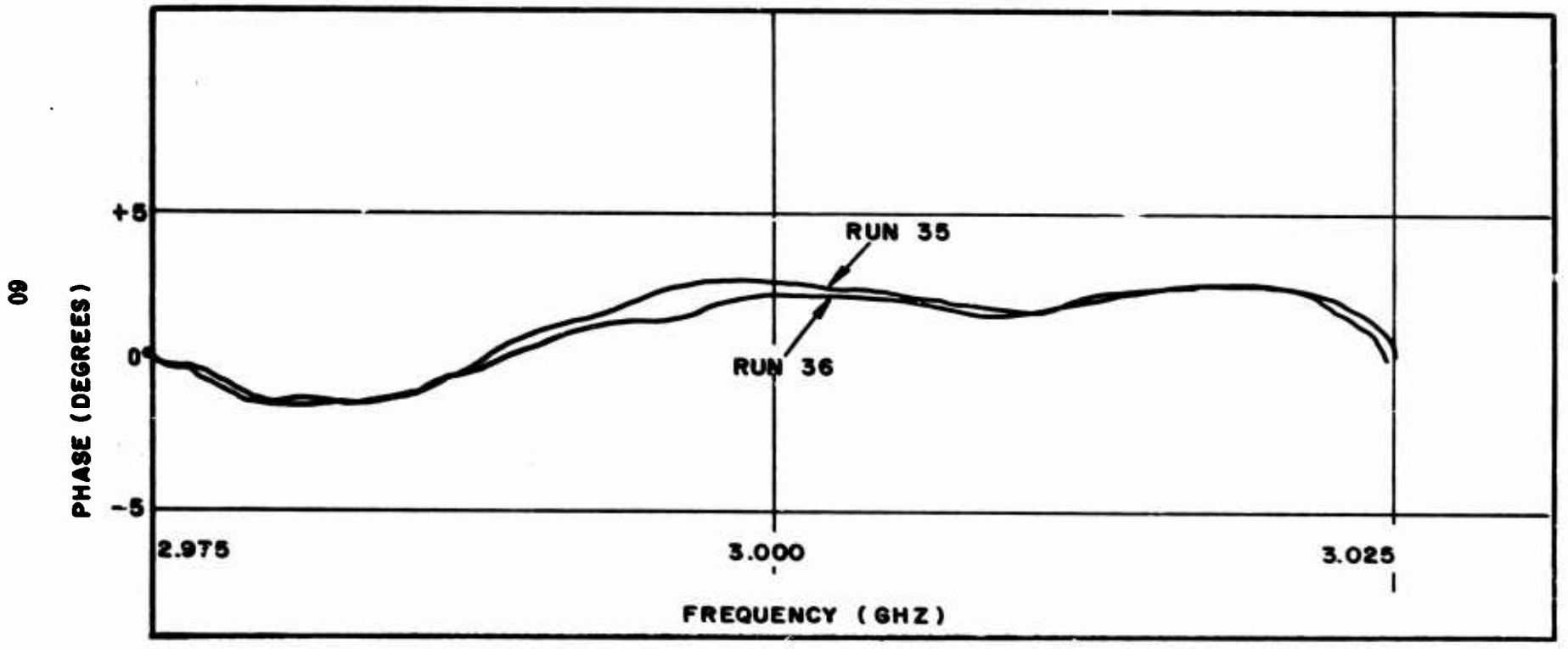

Figure 36. Phase vs. Frequency Characteristics of Transmitter Klystron. 12 January 1966. Klystron Cavities Tuned for Best Phase Response. Runs 35 and 36 were taken from a Recorder Presentation. VKG.

distortion was sinusoidal in nature with maximum peaks of ±3 degrees. One cycle of sinusoidal phase variation was observed over the 50 MHz operating frequency band. When a linear FM signal was transmitted through the transmitter, negligible distortion was observed on a coherent memory filter output display. Theoretical calculations also showed that the phase distortion of the transmitter after klystron tuning would have negligible effects on system performance. The circuit arrangement for transmitter tests was given previously in Figure 14.

Swept frequency phase measurements provided either a real time, or essentially real time, readout of phase data. This allowed a further improvement in phase, correcting the overall transmitter. By observing the phase vs. frequency characteristics of the overall transmitter and experimentally determining the phase sensitivity of the TWT (phase sensitivity with respect to changes in helix voltage), a voltage waveform was synthesized and applied to the helix of the TWT. In effect, a phase response similar in nature but opposite in sign to that of the overall transmitter is purposely introduced by way of the TWT. Ideally, the two phase responses cancel and the resulting phase response is linear.

Since the phase measurement system has some residual phase curvature, a residual test was first made, and the residual phase vs. frequency characteristics were recorded. The next step in phase correction was to synthesize a waveform to correct the phase vs. frequency response of the overall transmitter. When the residual phase vs. frequency characteristics and the overall transmitter phase vs. frequency characteristic were identical, the overall klystron had linear phase vs. frequency response with an absolute accuracy of $\pm .5^{o}$ across the operating frequency band.

The above method outlines a fast, accurate and easily implemented method for eliminating unwanted phase distortions.

C. Summary of Test Results

1. Double-Probe Slotted-Line Tests (Fixed Frequency Measurements):

Phase measurement accuracy of the double-probe slotted-line method of measuring phase was dependent, to a large degree, upon the device under test. Phase deviations due to the phase measurement system itself were less than ±1 degree but when the test device consisted of several active devices in cascade, repeated phase samples at a given fixed frequency differed by as much as 3.6 degrees. Data was not repeatable and the phase linearity of the device under test could not be adequately described. As the device under test became more complex in nature and more devices were cascaded, phase measurement errors became larger still.

Phase uncertainties, when measuring phase linearity by sampling the phase at fixed frequency points across an operating frequency band, were investigated. Data taken on traveling-wave tube amplifiers showed that the total phase shift through a traveling-wave tube amplifier is dependent upon power input drive level. Traveling-wave tube amplifiers should be operated at least 15 db below input saturation level to minimize phase shifts due to changes in input drive power. In making phase measurements at fixed frequencies, the input drive to traveling-wave tube amplifiers should be held constant for all test frequency points.

Phase instabilities of active devices also contribute to phase measurement error when measuring phase linearity at fixed frequency points across the operating frequency band. For traveling-wave tube amplifiers, variations in helix voltage cause unwanted phase shifts or phase instabilities. The phase sensitivity of two low noise X-band traveling-wave tube amplifiers was experimentally determined to be 12^{o}/volt and 10.4^{o}/volt with respect to helix voltage, while the phase sensitivity of a medium power X-band traveling-wave tube amplifier was 2.8^{o}/volt. Observed changes of helix voltage were ±.04 volts for the low noise TWT's and ±.2 volts for the medium power TWT. Helix voltage fluctuations can result in phase instability errors of $\pm.48^{o}$ and $\pm.42^{o}$ for the low noise TWT's and $\pm.56^{o}$ for the medium power TWT. In the worst case, when the errors are additive, phase instability error can be as large as $\pm1.46^{o}$. The rms error due to phase instability of the TWT's is $\pm.85^{o}$.

Tests were performed to ascertain whether the tracked null drifted with time. Since the double-probe slotted-line method utilizes null tracking to measure phase, a drifting null would introduce phase errors. When the test device was a receiver chain, null drifts with time introduced measured phase errors as large as 7.4 degrees at a given fixed frequency. Environmental room temperature changes also contributed to phase errors. Changes in environmental room temperature had a marked effect on null drifting.

After many precautions and many preliminary tests were made, acceptable data was obtained on a X-band receiver chain. Tests showed that the phase non-linearity of the receiver chain was within acceptable limits.

Phase linearity tests on the transmitter showed that the transmitter had excessive phase deviations. Phase non-linearity of the transmitter was as great as 26 degrees across the operating frequency band. By applying a phase correction voltage to the helix of the transmitter traveling-wave tube amplifier driver, the phase non-linearity of the transmitter was improved to a maximum of 2.25^{o} across the operating frequency band. Phase tests on the transmitter klystron showed that a large percentage of phase deviations of the transmitter were due to klystron phase distortion.

2. Phase-Discriminator and Detector Tests (Swept Frequency Measurements)

Phase measurement accuracy of the phase discriminator and detector method of measuring phase linearity was essentially independent of the device under test. Phase curvature and reflection interaction errors were eliminated from a phase vs. swept frequency measurements by a calibration process. Phase measurement error was a maximum of $\pm.5^{o}$.

Phase vs. frequency characteristic measurements on coaxial cable showed that coaxial cable has essentially linear phase vs. frequency response. Maximum phase deviations of 116-foot lengths of coaxial cable were less than $.3^{o}$, and these small deviations were due to interconnecting cable connectors. Frequency was swept across the operating frequency band.

Tests performed on a complex slave site receiver chain showed that phase non-linearity of the receiver chain was less than 5 degrees across a 60 MHz frequency

band. These results were obtained after the parametric amplifiers were tuned for most linear phase vs. frequency response, mismatch errors were minimized throughout the chain and various precautions were taken. Phase distortion was minimized and phase non-linearities were well within system requirements.

Phase linearity tests on the master site S-band r-f receiving chain showed that the master site receiving chain had a maximum phase non-linearity of several degrees across the operating frequency band. The chain consisted of an S-band parametric amplifier and two traveling-wave tube amplifiers in cascade. Phase distortion in the master site r-f receiving chain will have negligible effect on system performance.

The traveling-wave tube amplifier portion of the transmitter showed a maximum phase deviation of about 2 degrees across the signal frequency band. This deviation will have negligible effect on system performance.

Round-trip phase tests were conducted over a microwave link approximately 6-1/4 miles in length. Phase variations vs. time were recorded and provide some interesting results. Typical noise-like phase deviations of 3 degrees peak-to-peak magnitude were observed. The general phase pattern was somewhat sinusoidal in nature and showed about 1 cycle/minute phase variation. Equating phase variations to time delay variations across the microwave link (assuming that frequency is constant) gives a time delay variation of about ±.003 nanoseconds due to sinusoidal phase variations across the link. This test showed that the error involved due to time delay changes across the link will be very small during normal system operation.

Phase vs. frequency characteristic measurements on the transmitter klystron showed that the klystron had a maximum phase deviation of 16.8 degrees across the operating frequency band. After the seven cavities of the klystron were tuned for maximum amplitude flatness across the operating frequency band, maximum phase deviation was 7 degrees. When the klystron was tuned for most linear phase vs. frequency response across the operating frequency band, phase non-linearity was a maximum of 2.6 degrees. Tuning the klystron for minimum phase deviations resulted in a value of output power approximately 1 db lower than the maximum power output capability of the klystron. Varying beam voltage 1000 volts changed the phase characteristics of the klystron very little. Less than 1 degree maximum change was observed. Varying beam voltage did, however, change the time delay through the klystron. Varying the input drive level to the klystron had some effect on the phase response of the klystron, but the effect was not large. One test was made with the klystron in hard saturation, and another test was made with the klystron operating at an input drive level 2 db below that required to drive the klystron into saturation. The phase vs. frequency characteristics obtained had the same general shape. Maximum variation between the characteristics obtained was less than 2 degrees and the phase characteristics were within .5° over 70 percent of the signal frequency band. Varying magnet currents ±10 percent changed the phase response of the klystron less than 1.5 degrees across the frequency band.

Tests performed on the overall transmitter, after the klystron had been tuned for most linear phase vs. frequency response, showed a maximum phase deviation of ±3° across the operating frequency band. Phase distortion was sinusoidal in nature with maximum peaks of ±3°. One cycle of sinusoidal phase variation was observed over the

50 MHz operating frequency band. When a linear FM signal was transmitted through the transmitter, negligible distortion was observed on a coherent memory filter output display.

Initial tests on several S-band parametric amplifiers showed that individual parametric amplifiers had as much as 10 degrees peak-to-peak phase deviation across the signal frequency band. By tuning the bias voltages of the varactor diodes in the parametric amplifiers (which essentially determines the band pass of the amplifiers), phase deviations were improved to 1 degree peak-to-peak across the frequency band.

Using a phase correction unit, the phase non-linearity of the overall transmitter was corrected to give a linear phase vs. frequency response with an absolute accuracy of $\pm .5^{o}$ across the operating frequency band.

SECTION V
CONCLUSIONS

Phase vs. frequency characteristic data taken manually is time-consuming, inaccurate, and does not completely describe the phase linearity of the device under test.

Phase measurement accuracy of a manual phase measurement system that uses a slotted-line phase detector is seriously degraded when the test device consists of cascaded active devices. A manual phase measurement system that measures phase linearity by tracking a null is plagued by many problems. Although the phase measurement system itself may have been carefully designed and constructed to minimize phase errors, it does not necessarily follow that good data will be obtained using the phase measurement system. If the test device is a complex receiver chain that contains a number of cascaded active devices, a drifting of the tracked null with time is often experienced. This drift introduces an error into manual phase data which produces erroneous results and data is not repeatable. The effects of a drifting null can be minimized by using a technique devised for the measurements of this report.

Phase stability of a receiver chain is considerably improved when active devices in the system are supplied power from a regulated line source. In some cases, filtering is also necessary if line voltage transients exist.

Accuracy of ±1 degree is extremely difficult, if not impossible, to achieve when measuring the phase linearity of a complex receiver chain using fixed frequency phase samples obtained by means of a slotted-line phase detector.

Traveling-wave tube amplifiers should be operated at input power levels at least 15 db below input saturation to minimize phase shifts due to changes in input drive power. For manual phase measurements, input drive power of traveling-wave tube amplifiers should be held constant. The helix voltage of traveling-wave tube amplifiers was found to be the most critical voltage affecting phase stability.

Environmental room temperature should be maintained fairly constant for manual phase measurements. Drifting of the tracked null with time is dependent to a large degree upon temperature changes.

Regulated beam voltages of traveling-wave tube amplifiers are often derived from the collector supply by several stages of Zener diode shunt regulation. If the Zener diodes are voltage stabilized against ambient temperature changes by mounting the Zener diodes in a crystal oven, phase transients often occur when the oven switches on and off.

Accuracy of ±.5 degrees can be obtained for swept-frequency phase measurements using the phase measurement system discussed in this report. Phase curvature and reflection interaction errors may be eliminated from phase vs. swept frequency data by a calibration process.

Line voltage fluctuations can cause unwanted phase instabilities in high power klystron amplifiers. Beam voltages of high power klystrons and traveling-wave tube amplifiers should be very highly regulated to minimize phase instabilities.

Parametric amplifiers can be tuned for most linear phase vs. frequency response by tuning the varactor diode bias voltages. Maximum phase deviations were improved by a factor of ten without a loss in gain.

Swept frequency phase measurements can be used as a diagnostic tool in evaluating overall system performance. Mismatches that often escape detection in gain and band-pass measurements usually show up in phase linearity measurements.

Coaxial cable has very nearly linear phase vs. frequency response.

Time delay changes across the ASFIR microwave links will be very small during normal system operation. Equating phase changes to time delay changes, assuming frequency remains constant, showed a time delay change of less than ±.003 nano-seconds over a 7-minute time period.

High power klystron amplifiers can be mechanically tuned for most linear phase vs. frequency response.

Phase nonlinearities in a transmission or receiving r-f chain can be eliminated by means of a phase correction unit. Linear phase vs. frequency response with an absolute accuracy of ±.5^{o} was obtained.

System performance degradation due to phase distortion in the ASFIR system were negligible after all components were optimized for most linear phase vs. frequency response.

SECTION VI

REFERENCES

1. "Phase Characteristic Measurements of the Trinidad Tracker System," Contract AF30(602)-2253, Federal Scientific Corporation, RADC-TR-61-24, 23 December 1960, Unclassified, P. 16., AD 321 932.

2. Ibid, Chap. II.

3. Carson, J.R., "Building up of Sinusoidal Currents in Long Periodically Loaded Lines," B.S.T.J., 3 (1924) p. 558.

4. Rinkel, S., "Measurement of Phase," Handbook of Electronic Measurements, Vol. II, Contracts AF30(602)-677 and AF30(602)-1578, Polytechnic Institute of Brooklyn, RADC-TN-57-242B 1956, Unclassified, Section 7.40, AD 131151.

5. "Model 305 Direct Reading Phase Meter," Wiltron Company Instruction Manual, 1962, pp. 9-28.

6. Grace, V.K., "Phase Measurement Report," October 1964 Unpublished.

7. Reference 5, op. cit., p. 19.

8. Lacy, P., "Automated Measurement of the Phase Transmission Characteristics of Microwave Amplifiers," IEEE International Convention Record, 1963, pp. 119-125.

9. Reference 5, op. cit., p. 1.

10. Ibid, p. 14.

11. Phillips, E.N., "The Uncertainties of Phase Measurement," Microwaves, February 1965, pp. 14-21.

12. Reference 8, Lacy, P., op. cit., p. 121.

13. Reference 6, Grace V.K., op. cit., pp. 19-22.

14. Cohn, S.B. and Weinhouse, N.P., "An Automatic Microwave Phase-Measurement System," Microwave Journal, Vol. 7, February 1964, p. 49.

15. Ibid, p. 50.

16. Ibid, pp. 51-55.

17. Reference 1, op. cit., p. 3.

18. Amster, G.S. and Gordon, R.L., "Waveguide Performs Well as Dispersive Device," Electronic Design, 26 April 1965, p. 42.

19. "Technical Proposal to Furnish a Set of Traveling-Wave Tube Amplifiers," Watkins-Johnson Company, 29 March 1962.

20. Grace, V.K., op. cit., pp. 19-22.

21. Reference 6, Ibid, p. 15.

22. Instruction Manual for Precision Microwave Phase Measurement System, Contract AF30(635)-36414, 8 November 1965, Section 2.

UNCLASSIFIED

Security Classification

DOCUMENT CONTROL DATA - R & D

(Security classification of title, body of abstract and indexing annotation must be entered when the overall report is classified)

1. ORIGINATING ACTIVITY *(Corporate author)*
Rome Air Development Center (EMASE)
Griffiss Air Force Base, New York 13440

2a. REPORT SECURITY CLASSIFICATION
UNCLASSIFIED

2b. GROUP
N/A

3. REPORT TITLE
Microwave Phase Measurements on the Active Swept Frequency Interferometer Radar System

4. DESCRIPTIVE NOTES *(Type of report and inclusive dates)*
In-House

5. AUTHOR(S) *(First name, middle initial, last name)*
Vaughn K. Grace, Captain, USAF

6. REPORT DATE	7a. TOTAL NO. OF PAGES	7b. NO. OF REFS
August 1967	68	22

8a. CONTRACT OR GRANT NO.	9a. ORIGINATOR'S REPORT NUMBER(S)
N/A	RADC-TR-67-305
b. PROJECT NO. 6512	
c.	9b. OTHER REPORT NO(S) *(Any other numbers that may be assigned this report)*
d.	None

10. DISTRIBUTION STATEMENT
This document is subject to special export controls and each transmittal to foreign governments or foreign nationals, or representatives thereto may be made only with prior approval of RADC (EMLI), GAFB, NY 13440.

11. SUPPLEMENTARY NOTES	12. SPONSORING MILITARY ACTIVITY
None	Rome Air Development Center (EMASE) Griffiss Air Force Base, New York 13440

13. ABSTRACT

Many microwave systems currently in operation require strict control of the phase and gain characteristics of the system. The Active Swept Frequency Interferometer Radar System transmits a linear FM ramp to obtain range and angle information. If the transfer characteristics of the system transmission and receiving networks possess constant gain and linear phase variation over the signal frequency band, the linear FM ramp signal will pass through the system undistorted. If, however, the system possesses inadequate phase linearity, the signal suffers phase distortion which results in a loss of signal amplitude and range resolution.

The various methods of measuring phase linearity and associated errors are discussed, as well as results of actual tests conducted on the components of the experimental Active Swept Frequency Interferometer Radar. These tests include results with passive components, as well as active components such as TWTs and high power klystrons.

DD FORM 1 NOV 65 1473

UNCLASSIFIED

Security Classification

14. KEY WORDS	LINK A		LINK B		LINK C	
	ROLE	WT	ROLE	WT	ROLE	WT
Electromagnetic Wave Phenomenon						
Phase Measurement						
Phase Distortion						
Pulse Compression						